Sci

MDPI

Article

Antitumor Potential of *Moringa oleifera* Extract Against PC3 Prostate Cancer Cells Through IGF-1 Pathway Modulation

Francesca Mancuso [1,*], Cinzia Lilli [1], Catia Bellucci [1], Veronica Ceccarelli [1], Anna Stabile [1], Cristiana Gambelunghe [1], Ludovica Pugliese [1], Margherita Cecchetti [2], Giovanni Luca [1] and Tiziano Baroni [1]

[1] Department of Medicine and Surgery, University of Perugia, 06132 Perugia, Italy; cinzia.lilli@unipg.it (C.L.); catia.bellucci@unipg.it (C.B.); veronica.ceccarelli@unipg.it (V.C.); anna.stabile@unipg.it (A.S.); cristiana.gambelunghe@unipg.it (C.G.); ludovica.pugliese@tiscali.it (L.P.); giovanni.luca@unipg.it (G.L.); tiziano.baroni@unipg.it (T.B.)

[2] Cluster of Excellence on Cellular Stress Responses in Aging-Associated Diseases (CECAD), University of Cologne, 50674 Cologne, Germany; margherita.cecchetti@hotmail.it

* Correspondence: francesca.mancuso@unipg.it; Tel.: +39-0755858232

Abstract

Moringa oleifera is widely recognized for its pharmacological properties and has recently attracted interest for its potential anticancer effects. In this study, we investigated the in vitro activity of *Moringa oleifera* leaf extract on the human prostate cancer PC3 cell line, focusing on the insulin-like growth factor 1 receptor (IGF1R) signaling pathway, a central regulator of prostate cancer progression. PC3 cells were treated with *Moringa oleifera* extract, IGF-1, the IGF1R inhibitor NVP-AEW541, and their combinations. Cell migration, apoptosis, cell cycle distribution, gene expression, and protein regulation were evaluated using scratch assays, flow cytometry, RT-PCR, and Western blotting. Under our experimental conditions, *Moringa oleifera* extract was associated with reduced IGF1R expression and phosphorylation, together with decreased activation of downstream ERK/MAPK and AKT signaling pathways. These changes were accompanied by increased apoptosis, G0/G1 cell cycle accumulation, and reduced migratory capacity of PC3 cells. In addition, *Moringa oleifera* modulated the expression of genes involved in epithelial–mesenchymal transition, tumor progression, and extracellular matrix remodeling, suppressing pro-invasive markers while enhancing anti-metastatic factors. The extract also reduced the expression of bone metastasis–associated markers, including osteocalcin and alkaline phosphatase. Overall, these findings indicate that *Moringa oleifera* exposure is associated with modulation of IGF1R-related signaling and cellular programs relevant to aggressive prostate cancer. Further studies will be required to determine pharmacological feasibility and translational relevance.

Keywords: anticancer properties; IGF-1/IGF1R pathway; *Moringa oleifera*; PC3; prostate cancer

Check for updates

Academic Editors: Vasil Georgiev and Andrea Fuso

Received: 19 December 2025
Revised: 18 February 2026
Accepted: 26 February 2026
Published: 2 March 2026

Copyright: © 2026 by the authors. Licensee MDPI, Basel, Switzerland. This article is an open access article distributed under the terms and conditions of the Creative Commons Attribution (CC BY) license.

1. Introduction

Prostate cancer is one of the most frequently diagnosed malignancies and remains a leading cause of cancer-related mortality among men worldwide [1]. Despite significant advances in diagnosis and therapy, the management of advanced and metastatic prostate cancer remains a major clinical challenge. Conventional treatments, including androgen deprivation therapy, chemotherapy, and radiotherapy, often show initial efficacy but are limited by severe side effects and the emergence of resistance, leading to aggressive and therapy-refractory disease [2]. Consequently, the search for new therapeutic strategies,

especially those based on natural compounds with high efficacy and low toxicity, has become a research priority.

In vitro prostate cancer models are widely employed to investigate disease mechanisms and evaluate novel therapeutic agents. Among them, the human PC3 cell line is a well-established model of advanced and metastatic prostate cancer [3]. Derived from bone metastasis of a prostate adenocarcinoma, PC3 cells exhibit high aggressiveness, invasive and migratory capacity, and lack functional androgen receptors, making them ideal for studying androgen-independent cancer [4,5]. PC3 cells are also suitable for exploring alterations in key oncogenic pathways, including PI3K/Akt/mTOR [6], MAPK/ERK [7], and Wnt/β-catenin [8,9]. Their ability to induce bone metastases in vivo further supports their use for investigating tumor-bone microenvironment interactions [10].

Natural products have attracted growing attention for cancer prevention and therapy due to their diverse bioactivities and favorable safety profiles. *Moringa oleifera Lam.* (Moringaceae), commonly known as the "tree of life," is native to subtropical regions of Asia and Africa and has long been used for nutritional and medicinal purposes [11,12]. Phytochemical analyses have identified a wide variety of bioactive constituents, including glucosinolates, isothiocyanates (e.g., sulforaphane), flavonoids (e.g., quercetin, kaempferol), phenolic acids, and vitamins [12].

Extensive in vitro and in vivo studies have reported multiple biological activities of *Moringa oleifera* extracts, such as antimicrobial [13,14], antioxidant [15], anti-inflammatory, and anticancer effects [16–19]. Additionally, antiproliferative and pro-apoptotic effects have been observed in several tumor models [20–22]. Preliminary evidence also suggests that *Moringa oleifera* extracts can inhibit the growth and viability of prostate cancer cells [23]. However, the molecular mechanisms underlying these effects remain largely unexplored.

The insulin-like growth factor 1 (IGF-1)/IGF-1 receptor (IGF1R) axis is a major signaling pathway involved in prostate tumorigenesis [24]. It regulates multiple biological processes, including cell proliferation, survival, epithelial-mesenchymal transition (EMT), and metastasis. Alterations in IGF1R signaling promote tumor aggressiveness and resistance to therapy, making this pathway an attractive target for therapeutic intervention. Despite the extensive literature on *Moringa oleifera*, no studies have yet examined its potential interaction with the IGF-1/IGF1R system in prostate cancer.

To address this hypothesis, we adopted a multi-level experimental approach in which different molecular and functional endpoints were analyzed as interconnected readouts of IGF-1/IGF1R activity in prostate cancer cells.

Based on these considerations, we hypothesized that *Moringa oleifera* exerts antitumor effects in PC3 cells through modulation of the IGF-1/IGF1R signaling pathway. To test this hypothesis, we first characterized the ethanol extract of *Moringa oleifera* using gas chromatography–mass spectrometry (GC-MS). The cytotoxicity of the extract was then evaluated using the MTT assay to determine the optimal treatment concentration.

Subsequently, PC3 cells were treated with *Moringa oleifera* extract, IGF-1, the IGF1R inhibitor NVP-AEW541 hydrochloride, or their combinations. To assess the biological effects, we performed cell cycle and apoptosis analyses to evaluate cell proliferation and viability.

Considering that EMT, migration, and extracellular matrix (ECM) remodeling are central to metastasis and have been reported to be influenced by IGF-1/IGF1R signaling, we also investigated whether *Moringa oleifera* could counteract these processes. Specifically, we analyzed morphological changes, migration capacity through scratch assay, and the transcriptional expression of epithelial (occludin) and mesenchymal (fibronectin, vimentin, N-cadherin) markers.

In addition, we evaluated ECM-related proteolytic enzymes. MMP-2 and MMP-9 are widely recognized as major gelatinases involved in prostate cancer invasion and progres-

sion and have been functionally linked to integrin α2β1–mediated signaling pathways [25]. However, increasing evidence indicates that matrix metalloproteinase expression in prostate cancer is highly context-dependent and influenced by tumor stage and molecular background. In this regard, MMP-13 (collagenase-3) has been implicated in extracellular matrix remodeling and tumor progression, although its precise role in prostate cancer remains debated and controversial [26–28]. Therefore, we investigated whether *Moringa oleifera* could modulate MMP-13 expression in AR-negative PC3 cells, together with cathepsin B and the endogenous protease inhibitors cystatin A and B, to obtain a broader view of ECM remodeling balance.

To explore whether *Moringa oleifera* interferes with the IGF-1/IGF1R axis, IGF1R gene and protein expression were evaluated by qRT-PCR and Western blotting, respectively. In prostate cancer, the IGF-1/IGF1R signaling axis functionally cooperates with integrins to promote tumor cell adhesion, migration, epithelial–mesenchymal transition, and metastatic dissemination. In particular, the α2β1 integrin heterodimer is highly expressed in aggressive and bone-metastatic prostate cancer cells and has been shown to mediate IGF-1–dependent pro-migratory and pro-invasive responses. Accordingly, integrins α2 and β1 represent biologically relevant downstream effectors of IGF-1 signaling in prostate cancer progression and were therefore examined in this study to investigate whether *Moringa oleifera* interferes with IGF-1–driven oncogenic programs [29]. Moreover, we investigated the effect of *Moringa oleifera* on the osteogenic differentiation potential of PC3 cells by analyzing osteocalcin and alkaline phosphatase gene expression.

Finally, to better elucidate the molecular mechanisms underlying the observed effects, we assessed the impact of *Moringa oleifera* on key cancer-related signaling molecules, including ERK, AKT (by Western blotting), and c-Myc (by qRT-PCR).

2. Materials and Methods

2.1. Reagents

All reagents used, unless otherwise specified, were purchased from the following companies: Sigma-Aldrich Co. (St. Louis, MO, USA), GIBCO-ThermoFisher (Rome, Italy), Sial (Rome, Italy), Corning (New York, NY, USA), and Chemicon International (Temecula, CA, USA).

2.2. Preparation of Moringa oleifera Extract

Maceration with 70% ethanol is a widely used and efficient method for extracting phenolic and flavonoid compounds from *Moringa oleifera* leaves [30].

Two grams of *Moringa oleifera* leaf powder (Bionutra, Germany) were mixed with 24 mL of 70% ethanol and kept under continuous agitation at room temperature for 72 h. The mixture was centrifuged at 259 g for 20 min, and the supernatant was filtered. The extract was evaporated to dryness using Rotavapor (BÜCHI Labortechnik AG, Flawil, Switzerland). The dried residue was weighed to determine the extraction yield and was reconstituted in 70% ethanol to obtain a stock concentration of 250 mg/mL. The final concentrations used in the treatments were obtained by diluting the stock solution with culture medium.

2.3. GC-MS Analysis

The dried extract was derivatized with 50 µL MSTFA at 70 °C for 30 min, evaporated under nitrogen, reconstituted in 1 µL methanol, and injected into a GC-MS system.

Analytical determination was performed using an Agilent 8860 gas chromatograph (Agilent Technologies, Palo Alto, CA, USA) coupled to a 5977B mass spectrometer. Separation was achieved using an HP-5MS capillary column (30 m × 0.25 mm × 0.25 µm), operated with helium at a flow rate of 1 mL/min and temperature programming of 80 °C

for 1 min ramped at 8 °C/min to 300 °C and held for 5 min. The samples (1 µL) were injected into a split-splitless injector at 250 °C in the splitless mode (1 min). MS acquisition for unknown substances was performed in the full-scan mode in the range of 41–500 amu. Identification of analytes was performed using the NIST spectral library [31].

2.4. PC3 Cell Line and Culture Conditions

PC3 human prostate adenocarcinoma cells (ATCC; purchased from Experimental Zooprophylactic Institute of Lombardia and Emilia-Romagna, Brescia, Italy) were cultured in F-12K Nut Mix medium supplemented with 10% fetal bovine serum (FBS) and penicillin/streptomycin (1X). Cells were maintained at 37 °C with 5% CO_2. Morphological changes following treatments were monitored using an inverted optical microscope.

2.5. Scratch Assay

The scratch assay is a widely used in vitro method to assess cell migration [32]. PC3 (3×10^5 cells/well) were cultured for 72 h in 6-well plates until confluence. A scratch was performed using a sterile 200 µL pipette tip and wells were washed to remove debris. Cells were treated with *Moringa oleifera* extract at 50, 100, or 200 µg/mL, and the migration assay was monitored at defined time points. Quantitative analysis of distances was performed using ImageJ software version 1.54k (National Institutes of Health, Bethesda, MD, USA).

2.6. Cytotoxicity Assay

PC3 were seeded at 1×10^5 cells/well, for 72 h, in 96-well plates until confluence and exposed to *Moringa oleifera* extract at 50, 100, 200 or 300 µg/mL. Cell viability was assessed by 3-(4,5-dimethylthiazol-2-yl)-2,5-diphenyltetrazolium bromide (MTT test) [33]. To assess potential cytotoxic effects on non-tumorigenic cells, PNT2 prostate epithelial cells (ATCC; purchased from Experimental Zooprophylactic Institute of Lombardia and Emilia-Romagna, Brescia, Italy) were treated with increasing concentrations of *Moringa oleifera* extract under the same experimental conditions, and cell viability was evaluated as described above. Data were reported as mean ± SD of eight replicates obtained from three independent experiments.

2.7. Experimental Design

The experimental design was conceived to evaluate whether *Moringa oleifera* modulates IGF-1-dependent signaling and cellular responses. IGF-1 treatment was used to reproduce a pro-tumorigenic condition characterized by activation of the IGF-1/IGF1R axis, whereas combined treatments with *Moringa oleifera* were performed to assess its ability to counteract IGF-1-induced effects.

PC3 cells were seeded at 3×10^5 cells/well in 6-well plates and incubated for 72 h. The following experimental conditions were applied:

- PC3 (unexposed control PC3 cells/Ctrl).
- PC3 + 100 µg/mL *Moringa oleifera.*
- PC3 + 50 ng/mL IGF-I.
- PC3 + 1 µM NVP-AEW541 hydrochloride.
- PC3 + 1 µM NVP-AEW541 + 50 ng/mL IGF-I.
- PC3 + 100 µg/mL *Moringa oleifera* + 50 ng/mL IGF-I.
- PC3 + 100 µg/mL *Moringa oleifera* + 1 µM NVP-AEW541 + 50 ng/mL IGF-I.

NVP-AEW541 is a selective ATP-competitive IGF1R inhibitor that reduces tumor growth in multiple xenograft models [19]. It was added 1 h before the other treatments. Exposure times to *Moringa oleifera* were set at 15 min and 24 h to evaluate early and late responses.

2.8. Apoptosis Assay

Cell cycle progression was assessed using propidium iodide staining. The organization of the eukaryotic cell cycle and key transitions has been well documented [21]. Cells were fixed in 70% ice-cold ethanol for at least 30 min at 4 °C, washed with FACS buffer (PBS + 2% FBS), incubated with RNase A (100 µg/mL, 15 min), and stained with PI (50 µg/mL). DNA content was measured using a FACSCalibur flow cytometer (Becton Dickinson, Milan, Italy) equipped with 488- and 633 nm lasers. CellQuest software version 5.1 (Becton Dickinson, CA, USA) was used to quantify the distribution of cells in each cell cycle phase: sub-G1 (dead cells), G0/G1, S, and G2/M. Flow cytometric analysis was performed on ≥25,000 events/sample in triplicate [33].

2.9. Cell Cycle Analysis

Annexin V–FITC/PI staining was used to quantify apoptosis, as previously described [34]. Externalization of phosphatidylserine enables detection of apoptotic cells, whereas PI identifies cells with compromised membrane integrity [20]. Cells were harvested, washed, and resuspended in 1X binding buffer. Annexin V–FITC (5 µL) and PI (5 µL) were added, and samples were incubated for 5 min in the dark. The combination of AnV and PI allows the discrimination of four cell categories: viable cells (AnV−/PI−), early apoptotic cells (AnV+/PI−), late apoptotic cells (AnV+/PI+), and necrotic cells (AnV−/PI+). The sum of apoptotic cells was also calculated. Flow cytometry data acquisition was performed on a FACSscan Calibur equipped with 488- and 633 nm lasers and running CellQuest Software. A minimum of 10,000 events/sample were collected.

2.10. Real-Time Quantitative PCR (RT-qPCR)

Real-Time quantitative PCR was performed as previously described [35]. Total RNA was extracted using TRIzol reagent (Ambion by Life Technologies, Carlsbad, CA, USA). RNA concentration and purity were assessed spectrophotometrically at 260 nm. cDNA was synthesized using ALL-IN-ONE 5X RT MASTER MIX (ABM Inc., Richmond, BC, Canada) with 1 µg RNA per reaction (20 µL). cDNA was stored at −20 °C. qPCR was performed using BlasTaq™ 2X qPCR Master Mix (ABM Inc.). Primer concentration was 0.5 µM (Table 1). β-actin served as a reference gene. Relative expression levels were calculated using the ΔΔCt method (MxPro™ software version 1.71, Agilent Technologies, CA, USA).

Table 1. Primer sequences for PCR analyses.

mRNA	Sequences (5′–3′)	Product (bp)	GenBank Accession No.
ALP	Fw: CCGTGGCAACTCTATCTTTGG Rv: GCCATACAGGATGGCAGTGA	79	NM_00478.6
C-myc	Fw: GGCGAACACACAACGTCTTGGAG Rv: GCTCAGGACATTTCTGTTAGAAG	298	NM_002467.6
Cathepsin B	Fw: CTACAGCGTCTCCAATAG Rv: GAAGTCCGAATACACAGA	91	L_16510.1
Cystatin A	Fw: AAGGGGACCTACATGTTCTGG Rv: ATAGGGCAGGGCTAAAAAGG	150	NM_005213.4
Cystatin B	Fw: GGGACAAACTACTTCATCAA Rv: GAGGGAGAGATTGGAACA	76	NM_000100.4
Fibronectin	Fw: CGAGGAGAGTGGAAGTGTGAGAG Rv: GGGTGAGGCTGCGGTTGG	108	NM_212482.1

Table 1. *Cont.*

mRNA	Sequences (5′–3′)	Product (bp)	GenBank Accession No.
IGF1R	Fw: CAAGCCTGAGCAAGATGATTC Rv: GAACTTATTGGCGTTGAGGTATG	74	NM_001845.4
Integrin α2	Fw: GTAGTTGACAACACAAAACAAACAA Rv: AAATAAAATTTTGTTGGAATGAAGC	150	NM_002203.3
Integrin β1	Fw: TGCCGGGTTTCACTTTGC; Rv: GTGACATTGTCCATCATTTGGTAAA	70	NM_033668.1
MMP13	Fw: TTCCCAGTGGTGGTGATGAA Rv: CATGGAGCTTGCTGCATTCT	128	NM_002427.2
N-Cadherin	Fw: CATCATCATCCTGCTTATCCTTGT Rv: TTCTCCTCCACCTTCTTCATCA	148	M_34064.1
Occludin	Fw: GCACCAAGCAATGACATA Rv: CAATAATGAGCATAGACAGGAT	154	U_49184.1
Osteocalcin	Fw: AGCAAAGGTGCAGCCTTTGT Rv: GCGCCTGGGTCTCTTCACT	63	NM_199173.2
Vimentin	Fw: GCTAACTACCAAGACACTATT Rv: TAGGTGGCAATCTCAATG	134	NM_003380.5
β-actin	Fw: ACCTTCTACAATGAGCTGCG Rv: TCCATCACGATGCCAGTGGTA	197	NM_001101.3

2.11. Western Blotting

Western blotting analysis was performed as previously reported [36]. Briefly, cells were lysed in RIPA buffer on ice and centrifuged at 14,000× *g* for 20 min. Protein concentration was determined using the Bradford assay. Equal amounts of protein were separated by 4–10% Tris-Tricine SDS-PAGE and subsequently transferred onto nitrocellulose membranes (Bio-Rad, Hercules, CA, USA). Membranes were stained with Ponceau Red, washed, and blocked with 5% BSA. Membranes were incubated overnight at 4 °C with the following primary antibodies: rabbit anti-pospho-IGF1R (p-IGF1R, 1:1000, Cell Signalling), mouse anti-phospho-ERK1/2 (p-ERK1/2, 1:100, Millipore, MA, USA), rabbit anti-phospho-AKT (p-AKT, 1:1000, Cell Signalling), rabbit anti-phospho-p38 (p-p38, 1:100, Cell Signalling), rabbit anti-phospho-JNK (p-JNK, 1:100, Cell Signalling), rabbit anti-β-actin (actin, 1:1000, Cell Signalling). After washing, membranes were incubated for an additional 60 min with HRP-conjugated secondary antibodies: anti-rabbit IgG (1:5000) and/or anti-mouse IgG (1:5000, Santa Cruz Biotechnology Inc., Dallas, TX, USA). Immunoreactive bands were visualized using the ChemiDoc™ XRS+ imaging system with Image Lab™ software version 5.0 (Bio-Rad).

2.12. Statistical Analysis

All data are presented as mean ± standard deviation (SD) from at least three independent biological experiments. Statistical analyses were performed using one-way or two-way analysis of variance (ANOVA), as appropriate, followed by Dunnett's post hoc test for comparisons versus the corresponding unexposed control PC3 cells (Ctrl).

ANOVA was selected as a robust parametric method commonly applied in in vitro experimental studies based on independent biological replicates. Given the experimental design and sample size, normal distribution was assumed according to standard practice in cell-based assays.

Statistical analyses were conducted using GraphPad Prism version 10.6.0 (Dotmatics). Levels of significance are indicated as follows: * $p < 0.05$, ** $p < 0.01$ and *** $p < 0.001$ vs. Ctrl.

3. Results

3.1. Characterization of Moringa oleifera Extract

After MSTFA derivatization, the ethanolic extract of *Moringa oleifera* leaves was subjected to GC–MS analysis. Figure 1 shows the total ion chromatogram (TIC) acquired in full-scan mode (41–500 *m*/*z*). Mass spectra were compared with the NIST library to identify the major components. According to the GC–MS profile, saturated and monounsaturated fatty acids and their derivatives represented the majority of the detectable fraction of the extract. The principal compounds identified included tetradecanoic acid, methyl palmitate, palmitic acid, isopropyl palmitate, methyl stearate, methyl oleate, stearic acid, and glycerol 1-palmitate. A semi-quantitative evaluation based on peak-area normalization (area%) of the identified compounds was performed to enhance chemical definition and batch reproducibility. Supplementary Table S1 reports the relative abundance data. Stearic acid was the most abundant component (62.9% of the total normalized peak area), followed by isopropyl palmitate (18.2%), methyl oleate (7.4%), and palmitic acid (7.2%). All these compounds have been reported in the literature as having antitumor-activity [37–39]. The remaining constituents each represented less than 2% of the integrated signal. These data provide a reproducible compositional fingerprint of the lipid fraction detectable under the applied GC–MS conditions. Based on its predominance and consistent detection, stearic acid was designated as a pragmatic operational reference marker for batch-to-batch reproducibility within this analytical framework. This designation is intended for quality-control purposes and does not imply that stearic acid represents the sole or principal bioactive constituent of the extract.

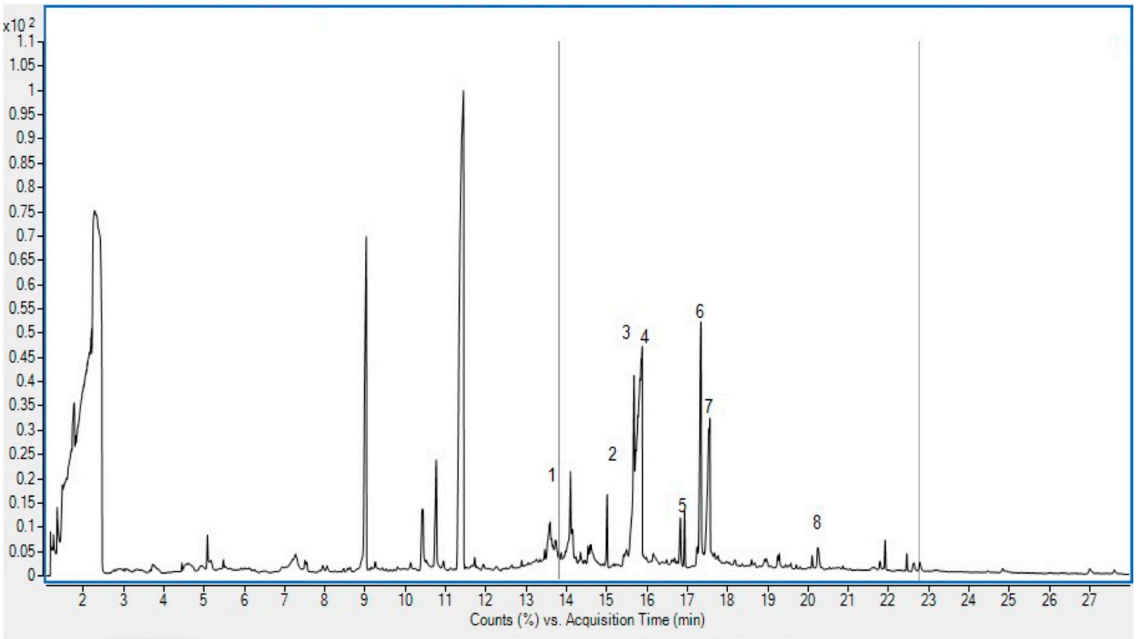

Figure 1. Chromatogram of *Moringa oleifera* solution. Representative GC–MS total ion chromatogram (TIC) of the *Moringa oleifera* leaf ethanolic extract after derivatization with MSTFA (full-scan acquisition, 41–500 *m*/*z*). Numbered peaks correspond to the major compounds identified by NIST library matching: (1) tetradecanoic acid; (2) hexadecanoic acid, methyl ester (methyl palmitate); (3) n-hexadecanoic acid (palmitic acid); (4) isopropyl palmitate; (5) methyl stearate; (6) 9-octadecenoic acid (Z)-, methyl ester (methyl oleate); (7) octadecanoic acid (stearic acid); and (8) glycerol 1-palmitate (1-monopalmitin). Grey lines are display cursors. Relative abundance (area%) of the identified peaks is reported in Supplementary Table S1.

3.2. Cytotoxicity Assay

To evaluate the cytotoxic potential of the *Moringa oleifera* extract, we first analyzed its effects on PC3 prostate cancer cells using the MTT assay, a standard test that measures cellular metabolic activity as an indirect indicator of cell viability. Approximately 50% of PC3 cells remained metabolically active and viable after treatment with the highest concentration of extract (300 µg/mL), indicating only mild cytotoxic effects compared with untreated control cells (Figure 2; * $p < 0.05$ and ** $p < 0.01$ vs. Ctrl).

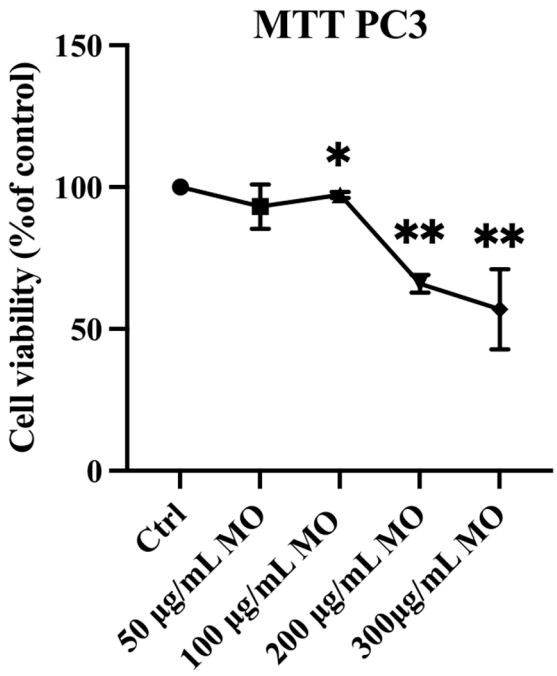

Figure 2. Cytotoxicity of *Moringa oleifera* extract on PC3 cancer cells. Cells were exposed to increasing concentrations of extract (50, 100, 200, and 300 µg/mL) for 24 h. Cell viabilities were measured via MTT assay. Data are presented as mean ± SD from three independent biological replicates. Statistical analysis was performed using one-way ANOVA followed by Dunnett's post hoc test (* $p < 0.05$ and ** $p < 0.01$ vs. Ctrl).

To preliminarily assess selectivity, viability experiments were also performed in the non-tumorigenic prostate epithelial cell line PNT2 under identical experimental conditions. Concentrations effective in PC3 cells (100–300 µg/mL) did not significantly reduce PNT2 viability, whereas a measurable reduction was observed only at markedly higher concentrations (approximately 1500 µg/mL) (Supplementary Figure S1).

3.3. Scratch Assay Analysis

To determine whether *Moringa oleifera* extract could influence the migratory capacity of PC3 cells, which underlies their highly metastatic behavior, we performed a scratch assay. PC3 cell monolayers were treated for 24 h with *Moringa oleifera* at 50, 100, and 200 µg/mL. Treatment reduced the migratory response of PC3 cells, as indicated by the inhibition of scratch closure compared with untreated monolayers (Figure 3, upper panels A–D). To quantify the extent of scratch recovery over time, channel widths were measured using ImageJ software and plotted relative to the distances measured at time 0 (Figure 3E). *Moringa oleifera* inhibited PC3 cell migration in a dose-dependent manner. Based on cytotoxicity and scratch assay results, a concentration of 100 µg/mL was selected for subsequent experiments.

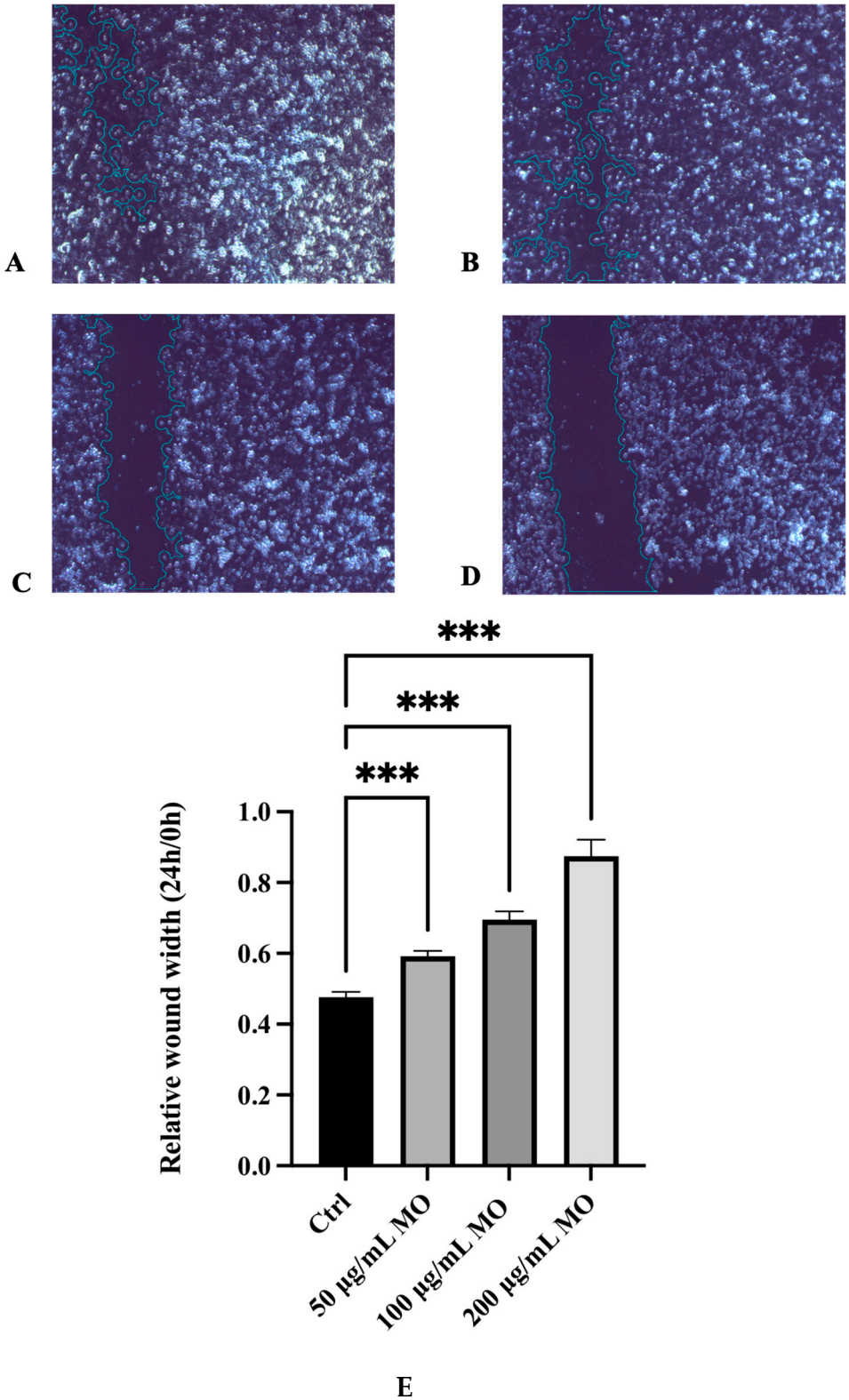

Figure 3. Bright-field image of the scratch test performed on PC3 cells. Treatments with *Moringa oleifera* extract: (**A**) Control, (**B**) 50 µg/mL, (**C**) 100 µg/mL, and (**D**) 200 µg/mL for 24 h. (4× original magnification). *Moringa oleifera* treatments inhibited the migration of PC3 prostate cancer cells in a dose-dependent manner. The channel widths relative to time zero were measured and plotted (panel (**E**)). Data are presented as mean ± SD from three independent biological replicates. Statistical analysis was performed using one-way ANOVA followed by Dunnett's post hoc test (*** $p < 0.001$ vs. Ctrl).

3.4. Morphology of Treated PC3 Cells

Light microscopy was used to assess morphological changes and variations in cell density in PC3 cells treated with 100 µg/mL *Moringa oleifera* extract, IGF-1, and NVP-AEW541 hydrochloride, alone or in combination, compared with untreated cells. Untreated PC3 cells displayed the typical spindle-shaped morphology and a confluent monolayer (Figure 4A). In contrast, *Moringa oleifera*-treated cells appeared more rounded, consistent with a stress-associated condition, and exhibited reduced monolayer density (Figure 4B). Cells treated with IGF-1 alone formed a confluent monolayer, maintaining their original spindle-shaped morphology and lacking the rounded appearance (Figure 4C). Micrographs from the other treatment conditions are reported in the Supplementary Material (Figure S2A–D).

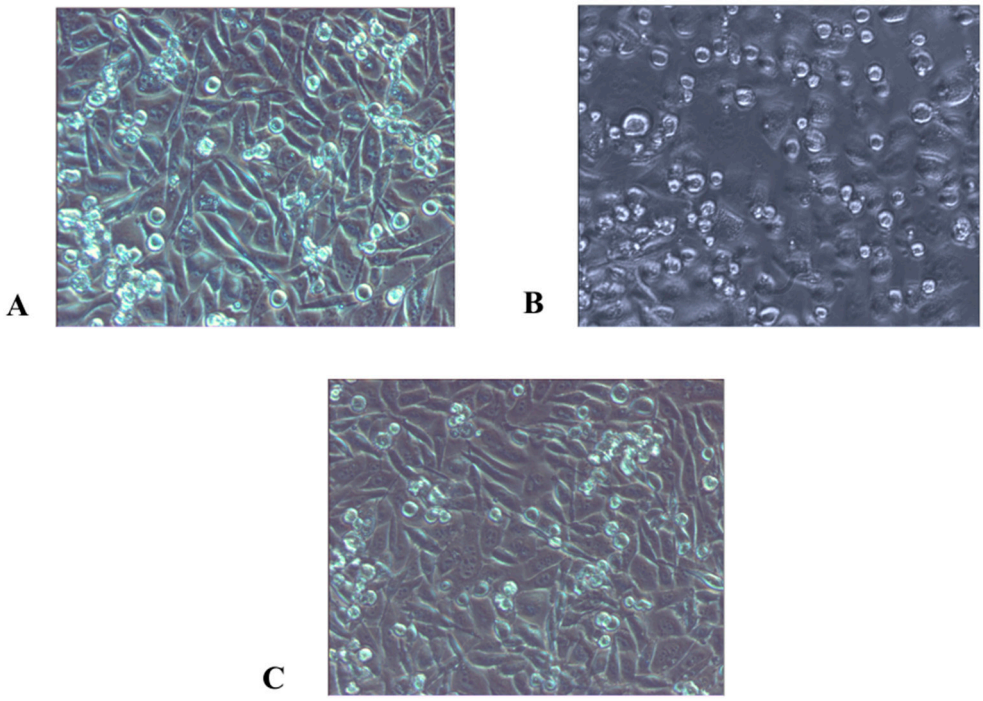

Figure 4. Light microscopy images of PC3 cells under different experimental conditions. (**A**) untreated PC3 cells, (**B**) PC3 cells treated with 100 µg/mL *Moringa oleifera* extract, (**C**) PC3 cells treated with 50 ng/mL IGF-1. Images are representative of three independent experiments, each performed in triplicate. Original magnification: 20×.

3.5. Effects of Moringa oleifera Alone and in Combination on PC3 Cell Cycle and Apoptosis

Given that *Moringa oleifera* inhibited PC3 cell migration and altered cell morphology, we next investigated whether the extract, alone or in combination, affected cell cycle distribution and cell death. Flow cytometry was used to analyze cell cycle progression, apoptosis, and necrosis.

Cell cycle analysis allowed us to quantify the percentage of cells in each phase. No statistically significant differences were observed in the percentage of cell death (subG1 phase) among treatments (Figure 5A and Figure S3A–G), indicating that the treatments did not induce increased necrosis or early apoptosis detectable in this fraction.

In contrast, a significant increase in the percentage of cells in the G0/G1 phase, indicative of quiescence, was observed in all samples containing *Moringa oleifera*, both alone (** $p < 0.01$ vs. Ctrl) and in combination (** $p < 0.01$ vs. Ctrl). No significant differences were detected in the IGF-1-treated sample (Figure 5B and Figure S3A–G).

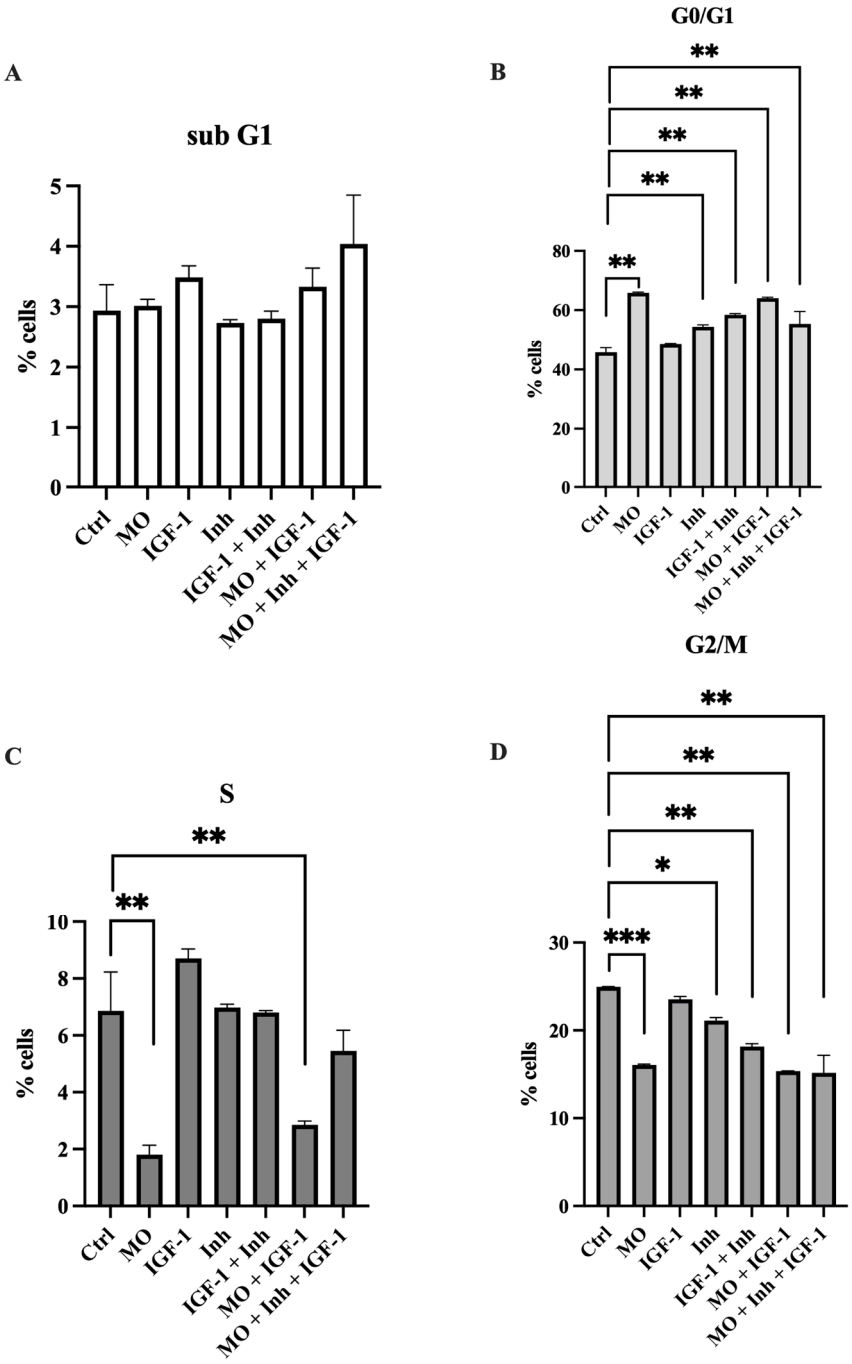

Figure 5. Cell cycle assay. (**A**) Percentage of cells in subG1 phase, (**B**) G0/G1, (**C**) S, and (**D**) G2/M in unexposed control PC3 cells (Ctrl) or after 24 h treated PC3 cells (MO = 100 µg/mL *Moringa oleifera*; IGF-1 = 50 ng/mL IGF-1; Inh = 1 µM NVP-AEW541 hydrochloride). Data are presented as mean ± SD from three independent biological replicates. Statistical analysis was performed using one-way ANOVA followed by Dunnett's post hoc test (* $p < 0.05$, ** $p < 0.01$ and *** $p < 0.001$ vs. Ctrl).

In the S phase, corresponding to DNA replication, a statistically significant reduction in the percentage of cells was observed after treatment with *Moringa oleifera* both alone and in combination with IGF-1 (** $p < 0.01$ vs. Ctrl). The sample treated with all three compounds did not show statistically significant differences (Figure 5C and Figure S3A–G).

A significant decrease in the percentage of cells in the G2/M phase was observed in all treated samples except those treated with IGF-1 alone (* $p < 0.05$, ** $p < 0.01$ and *** $p < 0.001$ vs. Ctrl). *Moringa oleifera* alone reduced the G2/M population to a greater extent than the other treatments (Figure 5D and Figure S3A–G).

Overall, analysis of cell cycle distribution based on DNA content showed an increase in the percentage of PC3 cells in G0/G1 (Figure S4A,B), accompanied by a decrease in the percentage of cells in S and G2/M phases (Figure S4A,B) following 100 µg/mL *Moringa oleifera* treatment compared with untreated controls (Ctrl).

Apoptosis was evaluated by flow cytometry (Figure 6). A statistically significant reduction in the percentage of viable cells was observed in all samples containing *Moringa oleifera* extract, due to a significant increase in total (early + late) apoptotic cells (** $p < 0.01$ vs. Ctrl). A statistically significant increase in late apoptotic cell death was also detected in IGF-1-treated samples following IGF1R blockade with NVP-AEW541 hydrochloride (Figure 6, ** $p < 0.01$ vs. Ctrl; Figure S5A–G). Taken together, these results indicate that treatment with *Moringa oleifera* alone or in combination with the other molecules tested influenced PC3 cell cycle progression and induced apoptosis, while IGF-1 alone did not produce comparable effects under our conditions.

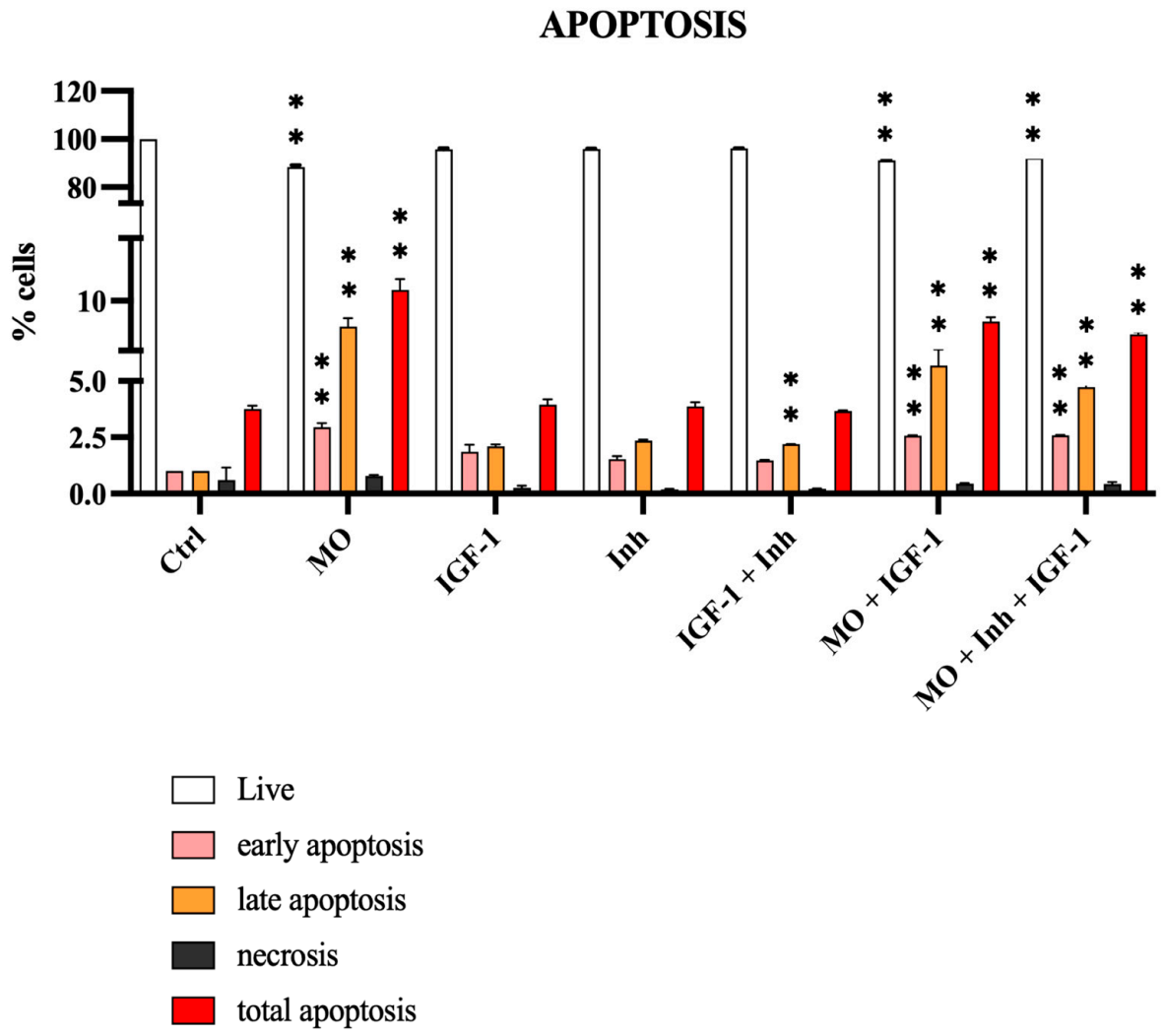

Figure 6. Assessment of apoptosis (early apoptosis—late apoptosis—total apoptosis), necrosis, and viable cells. *Moringa oleifera* (100 µg/mL) treatment alone or in combination (IGF-1 = 50 ng/mL IGF-1; Inh = 1 µM NVP-AEW541 hydrochloride) for 24 h induced both early and late apoptosis. Data are presented as mean ± SD from three independent biological replicates. Statistical analysis was performed using two-way ANOVA followed by Dunnett's post hoc test (** $p < 0.01$ vs. Ctrl).

3.6. Real-Time Polymerase Chain Reaction Analysis

Real-time PCR was performed to evaluate the effects of *Moringa oleifera* on the expression of key genes involved in cell functions and activities linked to cancer progression. Gene expression analysis was carried out on samples treated for 24 h. Data from the 15 min treatment were not included, as they did not provide relevant information for the endpoints examined.

3.6.1. Expression of IGF-1 Receptor Gene

To investigate whether *Moringa oleifera* acts on PC3 cells by interfering with the IGF-1 system, we analyzed IGF1R gene expression after treatment with *Moringa oleifera* extract alone and in combination with the other compounds. As shown in Figure 7A, *Moringa oleifera* alone induced a statistically significant decrease in IGF1R gene expression (** $p < 0.01$ vs. Ctrl). Neither IGF-1 nor NVP-AEW541 alone significantly modified IGF1R expression. In contrast, treatment with NVP-AEW541 followed by IGF-1, with or without *Moringa oleifera*, induced a statistically significant decrease in IGF1R gene expression (* $p < 0.05$ vs. Ctrl). The downregulation of IGF1R gene expression induced by *Moringa oleifera* extract indicates, for the first time, a link between *Moringa oleifera* and the IGF-1/IGF1R system, suggesting that this pathway may be one of the molecular targets of *Moringa oleifera*.

3.6.2. Expression of Integrins α2 and β1

Since the crosstalk between integrins and IGF-1 plays an important role in tumor onset and progression, we examined the effects of *Moringa oleifera* and the other treatments on the expression of integrins α2 and β1. Treatment of PC3 cells with *Moringa oleifera* alone decreased integrin α2 gene expression by approximately 50% compared with untreated controls (*** $p < 0.001$ vs. Ctrl), whereas IGF-1 alone stimulated integrin α2 expression by about 2.5-fold relative to control cells (*** $p < 0.001$ vs. Ctrl). This stimulatory effect of IGF-1 was much less pronounced when IGF-1 was administered in combination with *Moringa oleifera* or NVP-AEW541 (* $p < 0.05$ and *** $p < 0.001$ vs. Ctrl). Integrin α2 expression was decreased after treatment with all compounds (Figure 7B; *** $p < 0.001$ vs. Ctrl). Integrin β1 expression was also downregulated by *Moringa oleifera* alone and by all other treatments, except IGF-1, which showed only a non-significant trend toward upregulation (Figure 7C; ** $p < 0.01$ and *** $p < 0.001$ vs. Ctrl). These findings demonstrate that our *Moringa oleifera* extract has a significant downregulating effect on integrin gene expression. In particular, with regard to integrin α2, *Moringa oleifera* counteracts the IGF-1 signaling system, which tends to upregulate integrin α2 [40].

3.6.3. Expression of Epithelial-Mesenchymal Transition (EMT) Markers

To assess whether *Moringa oleifera* can counteract the pro-metastatic effects of IGF-1, we measured the expression of fibronectin, vimentin, and N-cadherin, recognized markers of epithelial-mesenchymal transition (EMT), a key event in metastasis during which mesenchymal markers increase and epithelial markers decrease. In PC3 cells treated with *Moringa oleifera* alone and in all combinations, fibronectin gene expression was significantly reduced compared with untreated controls after (Figure 7D; *** $p < 0.001$ vs. Ctrl). In contrast, statistically significant increases in fibronectin expression were detected in cells treated with IGF-1 (*** $p < 0.001$ vs. Ctrl) and, unexpectedly, in cells treated with the inhibitor alone. Notably, when PC3 cells were treated with both *Moringa oleifera* and IGF-1, the downregulating effect of *Moringa oleifera* predominated (Figure 7D). A similar pattern was observed for vimentin expression. *Moringa oleifera* alone induced a statistically significant decrease in vimentin gene expression, whereas IGF-1 alone induced a significant increase. The combined treatments did not markedly alter vimentin expression, except when all three

compounds were used together, which resulted in downregulation of vimentin (Figure 7E; * $p < 0.05$ and *** $p < 0.001$ vs. Ctrl). Treatment of PC3 cells with *Moringa oleifera* also induced a statistically significant reduction in N-cadherin gene expression compared with control cells, while IGF-1 induced only a non-significant increase (Figure 7E; * $p < 0.05$ vs. Ctrl). Combined treatment with *Moringa oleifera* and IGF-1 resulted in a non-significant decrease in N-cadherin expression (Figure 7E). As for epithelial markers, we analyzed the expression of occludin, a protein essential for maintaining cell–cell adhesion and epithelial integrity. As shown in Figure 8A, occludin expression was downregulated after IGF-1 treatment, whereas it was upregulated in cells treated with *Moringa oleifera* in combination with IGF-1 or with NVP-AEW541 hydrochloride compared with untreated controls (Figure 8A; * $p < 0.05$ vs. Ctrl).

Altogether, these data support the hypothesis that *Moringa oleifera* interferes with the IGF-1 system, counteracting its stimulatory effects on EMT. The dual role of *Moringa oleifera* in reducing cell invasion and reversing EMT is evident, highlighting its potential as a therapeutic agent to suppress prostate cancer metastasis.

3.6.4. Expression of c-Myc Oncogene

We next evaluated c-Myc gene expression in PC3 cells, as this oncogene is active in many types of cancer and is overexpressed in human prostate cancer [41]. A statistically significant reduction in c-Myc gene expression was observed in samples treated with *Moringa oleifera* alone and in all combinations, and in samples treated with NVP-AEW541 alone (Figure 8B; *** $p < 0.001$ vs. Ctrl). Treatment with IGF-1 alone resulted in a non-significant increase in c-Myc expression (Figure 8B).

3.6.5. Remodeling of Extracellular Matrix (ECM)

ECM remodeling in prostate cancer involves enzymes such as matrix metalloproteinases (MMPs) and proteases like cathepsins B, whereas cystatin A and cystatin B act as protease inhibitors, regulating enzymatic ECM degradation. In PC3 cells treated with IGF-1, cathepsin B gene expression was significantly increased (Figure 9A; * $p < 0.05$ vs. Ctrl). In contrast, treatment with *Moringa oleifera*, either alone or in all combinations, significantly reduced cathepsin B expression compared with untreated controls (Figure 9A; * $p < 0.05$ and ** $p < 0.01$ vs. Ctrl). Treatment of PC3 cells with *Moringa oleifera* led to a statistically significant decrease in MMP13 gene expression compared with untreated controls. Conversely, IGF-1 alone significantly increased MMP13 expression relative to control cells. Treatment with *Moringa oleifera* in combination with IGF-1 induced a non-significant decrease in MMP13 expression, whereas a significant decrease was observed in cells treated with *Moringa oleifera* plus inhibitor and IGF-1 (Figure 9B; *** $p < 0.001$ vs. Ctrl).

In contrast, transcriptional levels of the canonical gelatinases MMP-2 and MMP-9 were not significantly modulated under the tested experimental conditions. Regarding cystatin A and cystatin B, we observed statistically significant increases in the expression of both genes in all samples treated with *Moringa oleifera*, either alone or in combination with IGF-1 and the IGF1R inhibitor NVP-AEW541, compared with untreated PC3 cells (Figure 10A,B; *** $p < 0.001$ vs. Ctrl). IGF-1 treatment upregulated cystatin B expression but did not significantly affect cystatin A (Figure 10A,B; *** $p < 0.001$ vs. Ctrl).

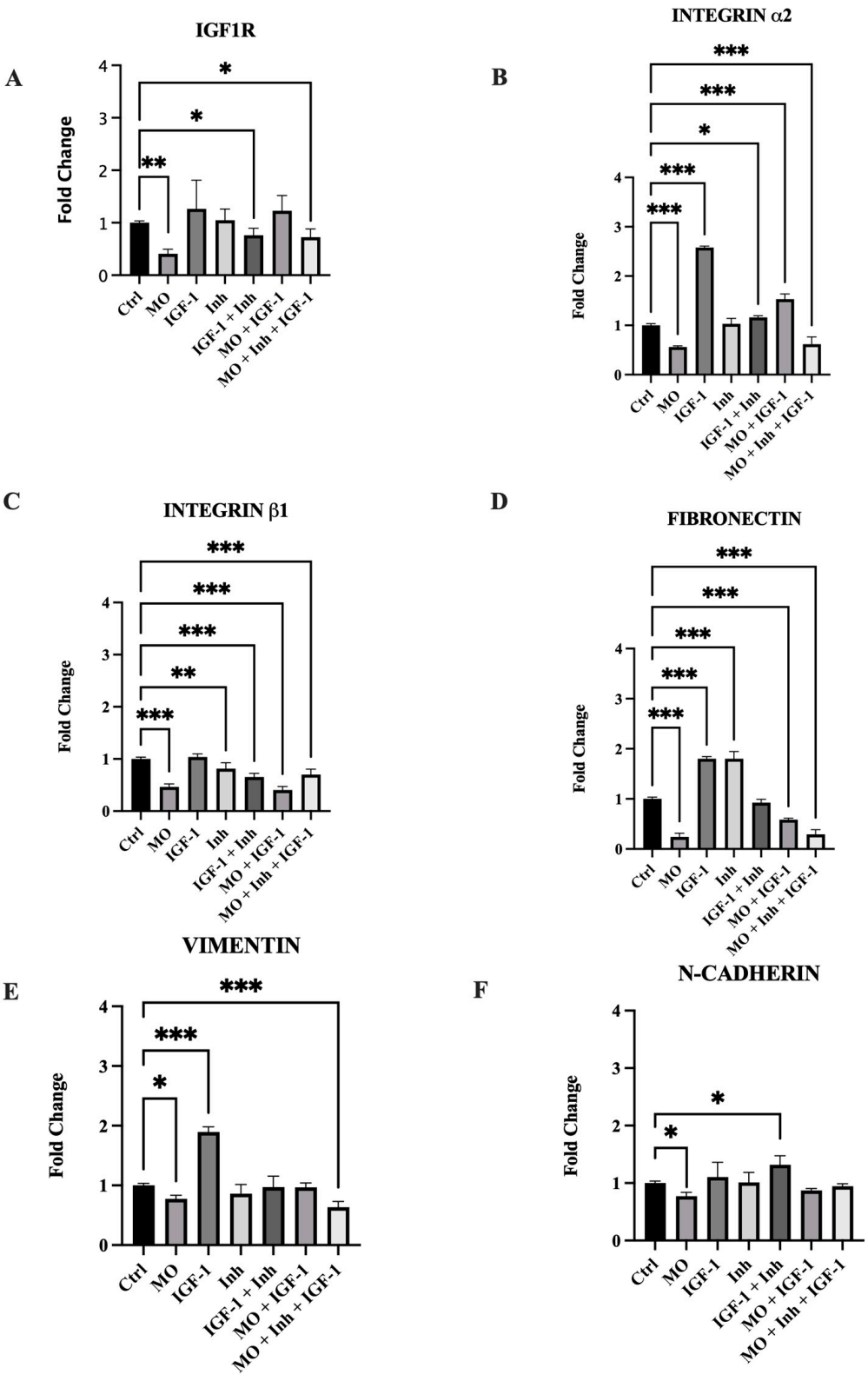

Figure 7. Real-Time PCR analysis. (**A**) Gene expression of IGF-1, (**B**) integrin α2, (**C**) integrin β1, (**D**) fibronectin, (**E**) vimentin and (**F**) N-cadherin in the different culture conditions. Abbreviations: Ctrl = unexposed PC3 control cells; MO = 100 μg/mL *Moringa oleifera*; IGF-1 = 50 ng/mL IGF-1; Inh = 1 μM NVP-AEW541 hydrochloride. Data are presented as mean ± SD from three independent biological replicates. Statistical analysis was performed using one-way ANOVA followed by Dunnett's post hoc test (* $p < 0.05$, ** $p < 0.01$ and *** $p < 0.001$ vs. Ctrl).

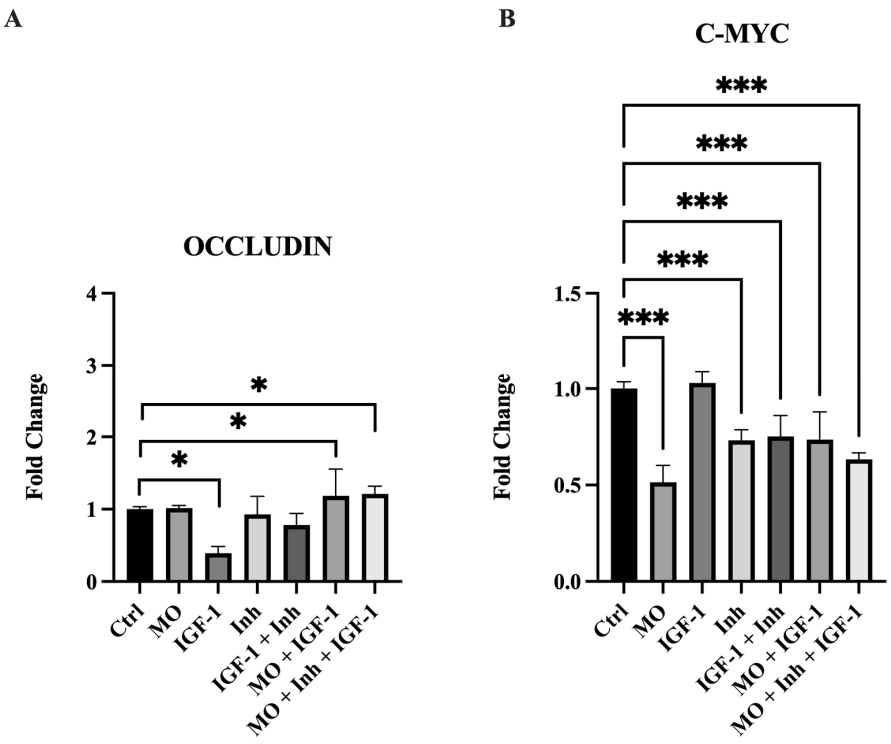

Figure 8. Real-Time PCR analysis. (**A**) Gene expression of occludin and (**B**) c-Myc in the different culture conditions. Abbreviations: Ctrl = unexposed PC3 control cells; MO = 100 µg/mL *Moringa oleifera*; IGF-1 = 50 ng/mL IGF-1; Inh = 1 µM NVP-AEW541 hydrochloride. Data are presented as mean ± SD from three independent biological replicates. Statistical analysis was performed using one-way ANOVA followed by Dunnett's post hoc test (* $p < 0.05$ and *** $p < 0.001$ vs. Ctrl).

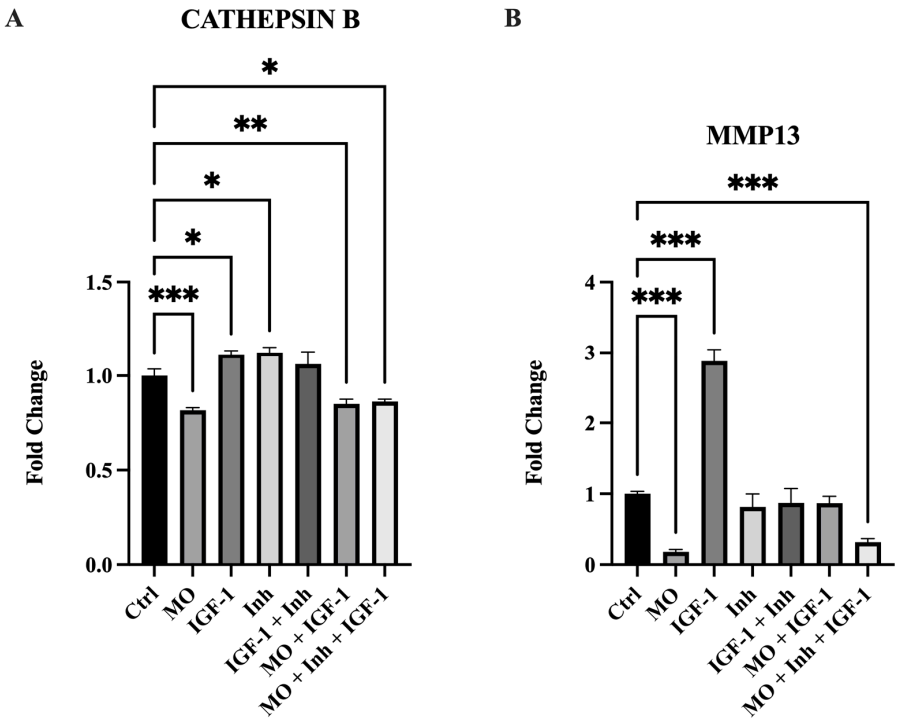

Figure 9. Real-Time PCR analysis. (**A**) Gene expression of Cathepsin B, and (**B**) MMP13 in the different culture conditions. Abbreviations: Ctrl = unexposed PC3 control cells; MO = 100 µg/mL *Moringa oleifera*; IGF-1 = 50 ng/mL IGF-1; Inh = 1 µM NVP-AEW541 hydrochloride. Data are presented as mean ± SD from three independent biological replicates. Statistical analysis was performed using one-way ANOVA followed by Dunnett's post hoc test (* $p < 0.05$, ** $p < 0.01$ and *** $p < 0.001$ vs. Ctrl).

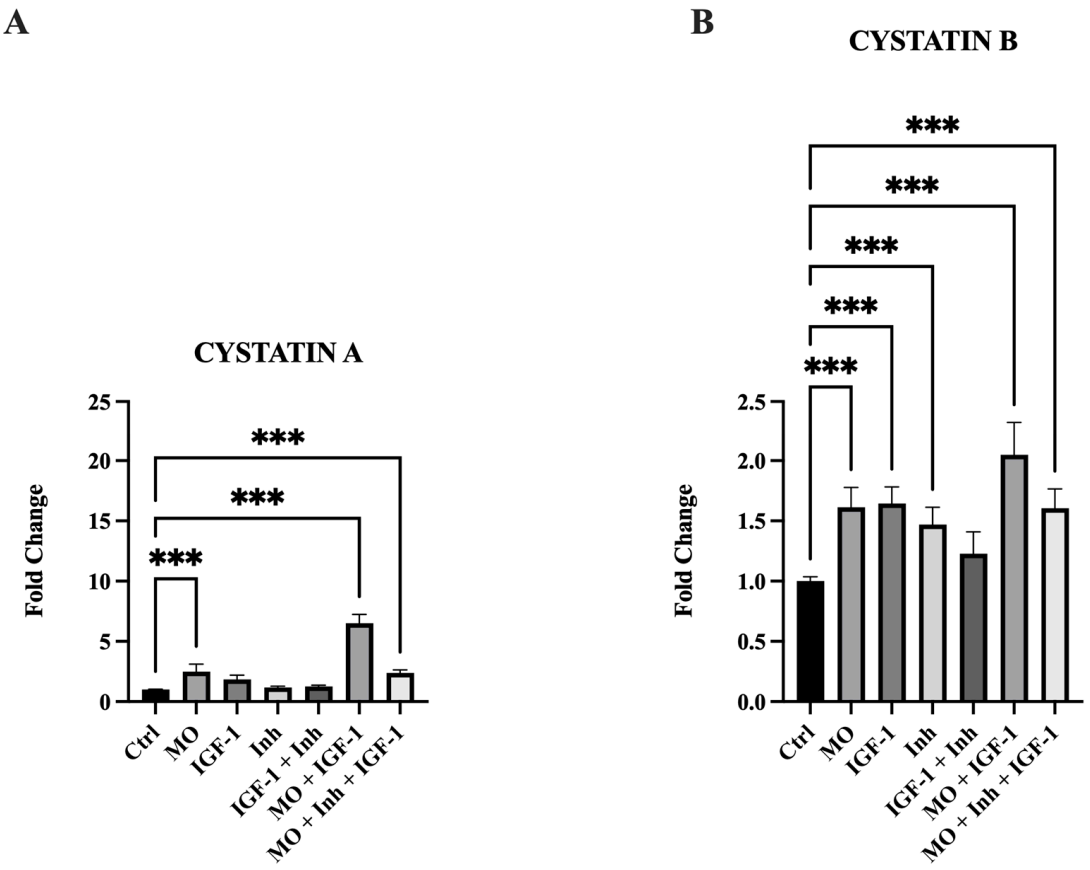

Figure 10. Real-Time PCR analysis. (**A**) Gene expression of Cystatin A, and (**B**) Cystatin B in the different culture conditions. Abbreviations: Ctrl = unexposed PC3 control cells; MO = 100 µg/mL *Moringa oleifera*; IGF-1 = 50 ng/mL IGF-1; Inh = 1 µM NVP-AEW541 hydrochloride. Data are presented as mean ± SD from three independent biological replicates. Statistical analysis was performed using one-way ANOVA followed by Dunnett's post hoc test (* $p < 0.05$, ** $p < 0.01$ and *** $p < 0.001$ vs. Ctrl).

3.6.6. Expression of Bone Phenotypic Genes

To investigate the effects of *Moringa oleifera* on the propensity of PC3 cells to form bone metastases, we evaluated the expression of osteocalcin and alkaline phosphatase, two biomarkers associated with bone metastases [10]. Treatment with *Moringa oleifera* alone induced a statistically significant reduction in osteocalcin gene expression compared with untreated cells. In contrast, IGF-1-treated PC3 cells showed a significant increase in osteocalcin expression (about three-fold versus Ctrl). Combined treatment with *Moringa oleifera* and IGF-1 did not modify osteocalcin expression levels relative to untreated cells; meanwhile, the combined treatments induced a statistically significant reduction (Figure 11A; ** $p < 0.01$ and *** $p < 0.001$ vs. Ctrl). Treatment with *Moringa oleifera* alone induced a statistically significant reduction in alkaline phosphatase gene expression compared with untreated cells. In contrast, IGF-1-treated PC3 cells showed a significant increase in alkaline phosphatase gene expression (about six-fold versus control; Figure 11B; * $p < 0.05$ and *** $p < 0.001$ vs. Ctrl). These findings indicate that *Moringa oleifera* reduces the bone metastatic potential of PC3 cells, in part by counteracting the stimulatory effects of IGF-1 on osteocalcin and alkaline phosphatase expression, and further underscore the link between *Moringa oleifera* effects and IGF-1 signaling.

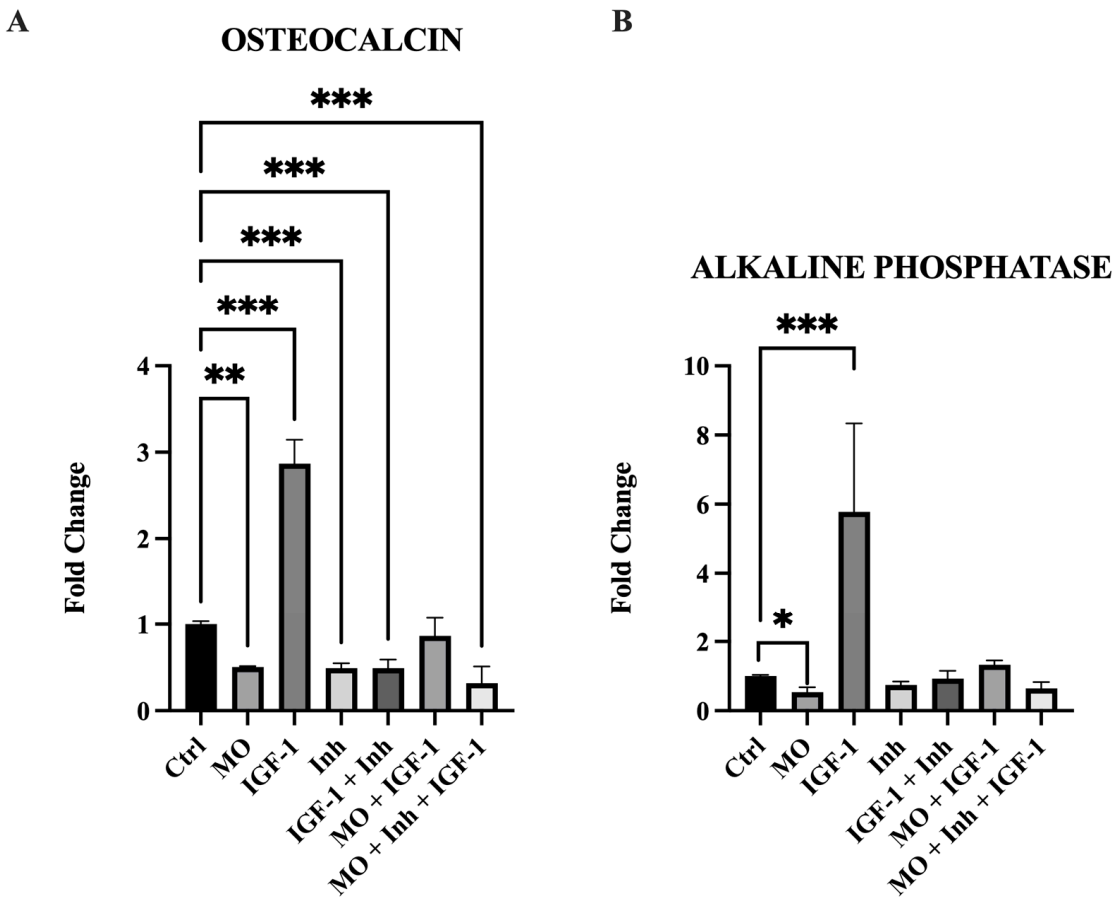

Figure 11. Real-Time PCR analysis. (**A**) Gene expression of osteocalcin, and (**B**) alkaline Posphatase in the different culture conditions. Abbreviations: Ctrl = unexposed PC3 control cells; MO = 100 µg/mL *Moringa oleifera*; IGF-1 = 50 ng/mL IGF-1; Inh = 1 µM NVP-AEW541 hydrochloride. Data are presented as mean ± SD from three independent biological replicates. Statistical analysis was performed using one-way ANOVA followed by Dunnett's post hoc test (* $p < 0.05$, ** $p < 0.01$ and *** $p < 0.001$ vs. Ctrl).

3.7. Western Blotting Analysis

We then assessed the expression of proteins involved in key intracellular signaling pathways, including IGF-1/IGF1R, MAPK/ERK1/2, and PI3K/AKT, by Western blotting in PC3 cells after 15 min and 24 h of treatment. These points were chosen to evaluate both early signaling events and possible effects on protein synthesis. Data from the 15 min treatment were not included, as they did not provide relevant information for the endpoints examined.

24 h Treatment Analysis

After 24 h of treatment, a statistically significant reduction in the IGF1R phosphorylation index was observed in samples treated with *Moringa oleifera*, with NVP-AEW541 hydrochloride, and with the combination NVP-AEW541 + IGF-1 (IGF-1 + Inh) (Figure 12A; * $p < 0.05$ and *** $p < 0.001$ vs. Ctrl). For the MAPK pathway, ERK 1/2 phosphorylation (p-ERK 1/2/actin) was significantly reduced in all treatments except IGF-1 compared with untreated cells (Figure 12B; *** $p < 0.001$ vs. Ctrl).

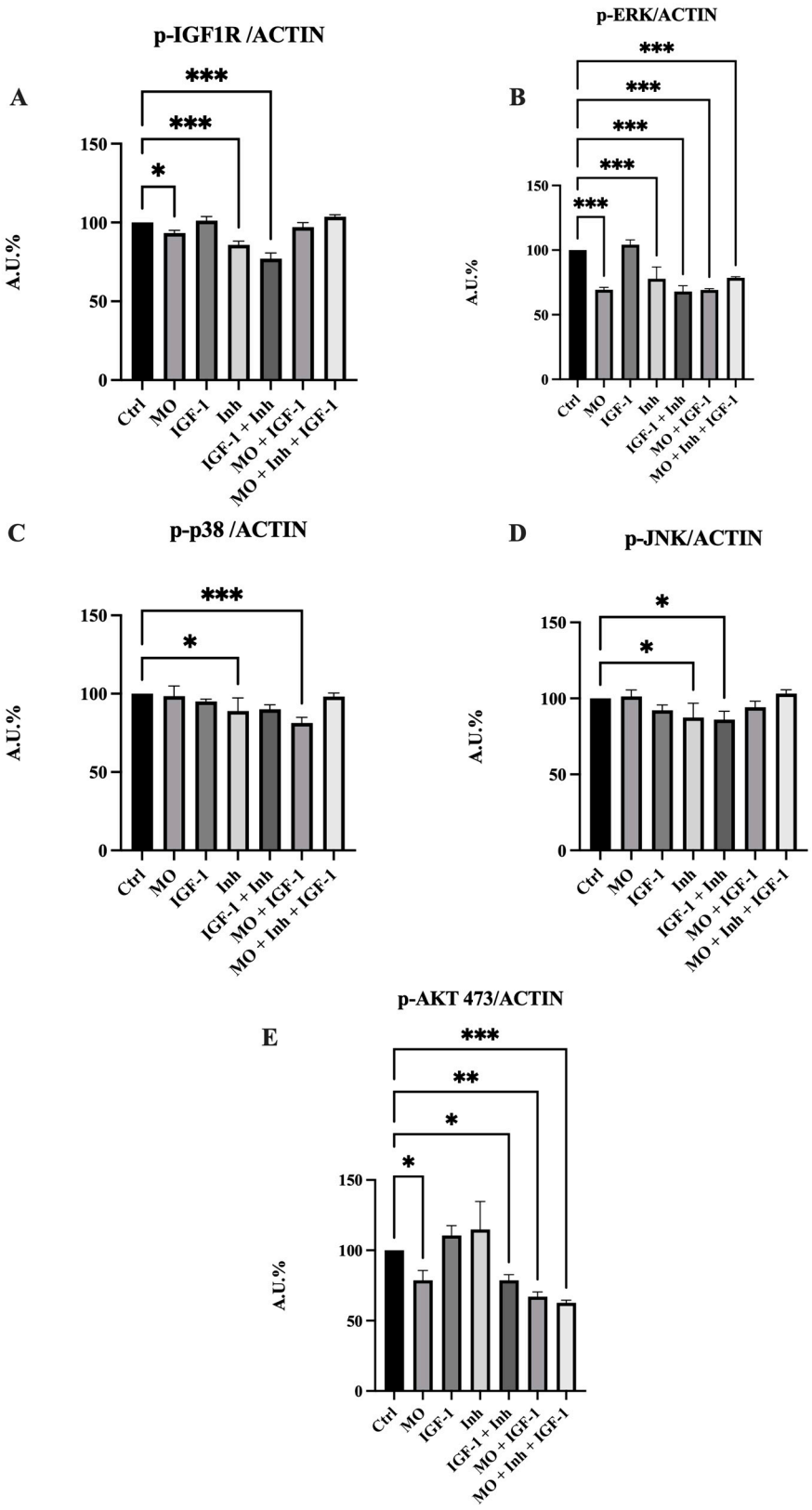

Figure 12. *Cont.*

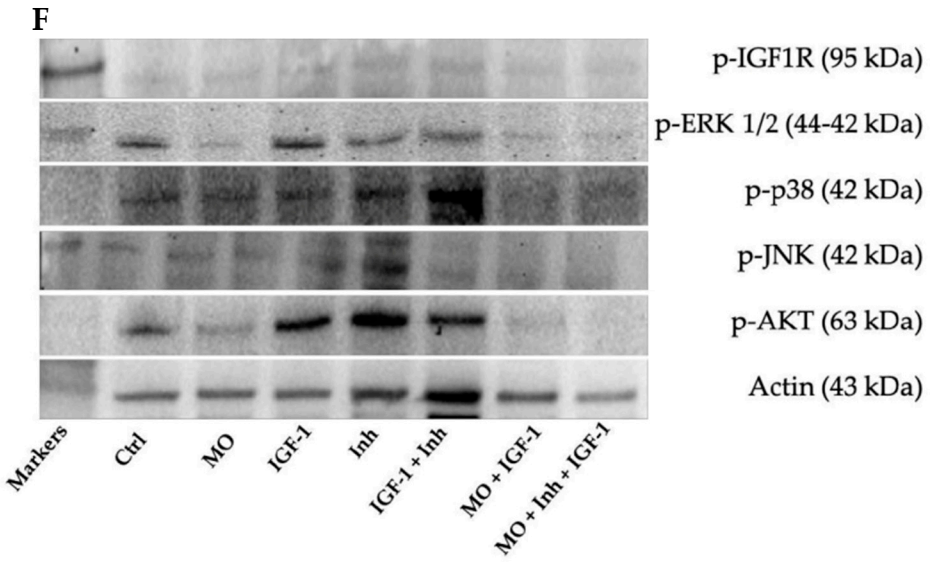

Figure 12. Western Blotting analysis. Densitometric analysis of p-IGF1R (95 kDa, panel (**A**)), p-ERK (44–42 kDa, panel (**B**)), p-p38 (42 kDa, panel (**C**)), p-JNK (42 kDa, panel (**D**)), p-AKT (63 kDa, panel (**E**)), and relative Immunoblotting images (panel (**F**)). Treatments were performed for 24 h, after pre-incubation with the IGF-1 receptor inhibitor 1 h prior in the designated samples. Abbreviations: Ctrl = unexposed PC3 control cells; MO = 100 μg/mL *Moringa oleifera*; IGF-1 = 50 ng/mL IGF-1; Inh = 1 μM NVP-AEW541 hydrochloride. Data are presented as mean ± SD from three independent biological replicates. Statistical analysis was performed using one-way ANOVA followed by Dunnett's post hoc test (* $p < 0.05$, ** $p < 0.01$ and *** $p < 0.001$ vs. Ctrl).

For p38, a statistically significant reduction in p38 phosphorylation (p-p38/actin) was observed with *Moringa oleifera* plus IGF-1 and with the inhibitor alone, compared with the untreated control (Figure 12C; * $p < 0.05$ and *** $p < 0.01$ vs. Ctrl, respectively).

JNK phosphorylation (p-JNK/actin) was significantly decreased in PC3 cells treated with NVP-AEW541 hydrochloride alone or in combination with IGF-1 compared with untreated controls (Figure 12D; * $p < 0.05$ vs. Ctrl). Treatment of PC3 cells with *Moringa oleifera*, either alone or in combination with other treatments, resulted in a statistically significant reduction in AKT phosphorylation (p-AKT/actin) at Ser473 compared with control cells (Figure 12E; * $p < 0.05$, ** $p < 0.01$ and *** $p < 0.001$ vs. Ctrl). A similar decrease in AKT phosphorylation was observed following IGF-1 treatment in the presence of the IGF1R inhibitor (Figure 12E; * $p < 0.05$ vs. Ctrl).

In exploratory experiments conducted at a lower concentration (50 μg/mL), comparable modulation of IGF1R expression and downstream signaling pathways (ERK and AKT phosphorylation) was not observed.

Overall, these findings indicate that *Moringa oleifera* exposure is associated with modulation of signaling cascades downstream of IGF1R under the present experimental conditions.

4. Discussion

In this study, we report for the first time that *Moringa oleifera* ethanolic extract may exert antitumour activity in PC3 prostate cancer cells by modulating the IGF-1/IGF1R signaling axis, a pathway known to be involved in prostate tumorigenesis [24,29]. Although numerous pharmacological properties of *Moringa oleifera* have already been described, including antioxidant, anti-inflammatory, and anticancer effects [12,18,21], no previous work has evaluated its possible interaction with the IGF-1/IGF1R system in prostate cancer. Our findings suggest that the anticancer potential of *Moringa oleifera* could include modulation of the IGF-1/IGF1R axis and that prostate cancer therapy may benefit from the identification of Moringa-derived molecules

targeting this pathway. In this context, the different experimental endpoints analyzed in the present study could provide complementary information on distinct, yet interconnected, aspects of IGF-1/IGF1R-associated tumor progression.

Chemical analysis by GC/MS revealed that the extract contains saturated and monounsaturated fatty acids and derivatives such as tetradecanoic acid, palmitic acid, isopropyl palmitate, methyl oleate, stearic acid, and 1-monopalmitin. Several of these molecules are known to possess intrinsic anticancer activities [37–39], supporting the biological plausibility of the effects observed in PC3 cells. Functional assays showed that the extract reduced PC3 viability in a dose-dependent manner, with ~50% metabolically active cells at 300 μg/mL, indicating mild but significant cytotoxicity consistent with earlier observations obtained using Moringa extracts or purified isothiocyanates [20,21]. Likewise, the extract impaired PC3 cell migration in a dose-dependent fashion, confirming a previous study reporting that Moringa alkaloids inhibit PC3 proliferation and motility [23]. Based on dose–response analyses, 100 μg/mL of Moringa oleifera was selected for mechanistic investigations, as this concentration elicited consistent phenotypic and molecular changes while preserving metabolic activity and avoiding overt nonspecific cytotoxicity, as confirmed by MTT assay. Exploratory experiments conducted at lower concentrations (e.g., 50 μg/mL; unpublished data) did not demonstrate comparable modulation of the investigated molecular and signaling endpoints, further supporting 100 μg/mL as the minimal concentration capable of inducing reproducible pathway-associated changes under the present experimental conditions. Accordingly, this concentration should be regarded as a proof-of-concept in vitro setting rather than a direct surrogate of achievable in vivo exposure levels.

Morphological evaluations revealed that Moringa-treated PC3 cells became rounded and exhibited reduced monolayer density, consistent with stress and decreased adhesion, whereas IGF-1 maintained the spindle-shaped morphology characteristic of the untreated control, in line with its well-established pro-survival and pro-proliferative effects [42,43]. These contrasting responses are compatible with an antagonistic interplay between IGF-1 signaling and *Moringa oleifera* activity. Flow cytometric analyses showed that treatment with *Moringa oleifera*, either alone or in combination with IGF-1, induced a redistribution of PC3 cells within the cell cycle, characterized by an increase in the G0/G1 population and a reduction in S- and G2/M-phase cells, together with an increase in apoptotic cells [20]. IGF-1 alone did not significantly modify cell cycle distribution, showing only a non-significant trend toward an increase in S-phase cells, in agreement with its reported role in sustaining proliferative signaling rather than inducing cell cycle arrest [44,45]. In contrast, blockade of IGF1R in the presence of IGF-1 resulted in a partial accumulation of cells in G0/G1 and G2/M phases, consistent with previous reports describing cell cycle perturbations following IGF1R inhibition [45,46]. Notably, these effects were more pronounced when IGF-1 was combined with *Moringa oleifera*. This observation suggests that the activity of *Moringa oleifera* is not limited to selective IGF1R inhibition but could involve additional mechanisms affecting cell cycle regulation and apoptotic pathways associated with IGF-1 signaling, potentially through modulation of downstream pathways such as AKT and ERK [7].

One of the most relevant findings of our study is the marked downregulation of the IGF1R gene expression induced by *Moringa oleifera*, either alone or in selected combinations. Because IGF1R overexpression drives proliferation, survival, and metastasis in prostate cancer [8], its suppression may hold considerable therapeutic relevance. Alongside IGF1R, the extract also reduced integrins α2 and β1, whose interplay with IGF-1 signaling is central to tumour adhesion, migration, and progression [29,40]. As expected, IGF-1 upregulated integrin α2 expression, but this effect was markedly weakened when IGF-1 was co-administered with *Moringa oleifera*, supporting the notion that the extract could interfere with IGF-1-driven motility programs. Accordingly, changes in integrins α2 and β1 could

reflect the ability of *Moringa oleifera* to modulate IGF-1-dependent adhesion and migration pathways in prostate cancer cells.

Given the importance of epithelial-mesenchymal transition (EMT) in prostate cancer progression, we examined the expression of fibronectin, vimentin, and N-cadherin [47–49]. *Moringa oleifera* consistently downregulated these mesenchymal markers, while IGF-1 strongly induced fibronectin and vimentin, confirming its EMT-promoting role [50]. When *Moringa oleifera* and IGF-1 were combined, the extract maintained its suppressive effect, indicating its ability to override IGF-1-mediated EMT induction. In contrast, the epithelial marker occludin, whose repression enhances tumour invasiveness [51], was preserved or increased by *Moringa oleifera* in combination treatments and downregulated by IGF-1 alone. These results collectively reinforce the anti-metastatic potential of *Moringa oleifera* and its capability to counterbalance IGF-1-induced EMT programs.

The extract also reduced expression of the oncogene c-Myc, frequently upregulated in prostate cancer [41]. Since c-Myc controls proliferation, EMT, metabolism, and immune evasion [52], its downregulation may contribute to the multifaceted antitumour effects observed.

Furthermore, *Moringa oleifera* modulated the expression of genes involved in extracellular matrix remodeling, reducing cathepsin B and MMP13 while upregulating the protease inhibitors cystatin A and cystatin B. Since cathepsin B and MMP13 are associated with tumor invasion and metastatic progression [53,54], whereas cystatins counteract ECM degradation [55], this transcriptional pattern supports a shift toward a less invasive phenotype. In contrast, IGF-1 increased cathepsin B and MMP13 expression, reinforcing its pro-invasive role.

MMP-13 (collagenase-3), implicated in collagen type I degradation and tumor progression, has been proposed as a context-dependent mediator of prostate cancer aggressiveness [26–28]. Although MMP-2 and MMP-9 are classically regarded as key gelatinases involved in prostate cancer invasion and linked to integrin α2β1–mediated signaling [25], under our experimental conditions, their expression was not significantly affected by *Moringa oleifera*. This suggests that the anti-migratory effects observed in PC3 cells may rely on alternative ECM remodeling mechanisms rather than canonical gelatinase suppression. In this regard, the marked downregulation of integrins α2 and β1 may represent a complementary mechanism contributing to reduced invasive behavior independently of MMP-2 and MMP-9 transcriptional modulation.

In addition, *Moringa oleifera* decreased the expression of osteocalcin and alkaline phosphatase, two biomarkers associated with prostate cancer bone metastasis [10,56], whereas IGF-1 markedly upregulated them. These findings further support the ability of *Moringa oleifera* to attenuate IGF-1–driven invasive and bone-metastatic programs in PC3 cells.

Western blot analyses corroborated these transcriptional and phenotypic observations. At 24 h, *Moringa oleifera* reduced IGF-1R phosphorylation, therefore demonstrating that *Moringa oleifera* interferes either with upstream and downstream regulatory mechanisms in the IGF-1/IGF1R pathway. Downstream mediators of survival and metastasis, including ERK1/2, p38, and AKT, also exhibited reduced phosphorylation following treatment, confirming inhibition of key pathways associated with tumour progression [7,57–60]. In particular, the strong inhibition of AKT phosphorylation is noteworthy given its association with poor prognosis in prostate cancer [60]. Collectively, these molecular changes demonstrate that *Moringa oleifera* disrupts IGF1R-associated signaling cascades at multiple levels, contributing to apoptosis, impaired proliferation, and reduced metastatic traits.

To preliminarily assess selectivity, viability experiments were conducted in the non-tumorigenic prostate epithelial cell line PNT2. Under the same experimental conditions,

concentrations effective in PC3 cells (100–300 μg/mL) did not induce significant cytotoxicity in PNT2 cells, whereas a reduction in viability was observed only at markedly higher concentrations (approximately 1500 μg/mL). Although limited to metabolic viability assessment, these findings suggest a differential sensitivity between malignant and non-tumorigenic prostate cells under the tested conditions. Nevertheless, a comprehensive evaluation of the therapeutic window and pathway-specific modulation in normal epithelial models will require dedicated mechanistic studies.

This study has some limitations. The mechanistic analyses were performed in a single prostate cancer cell line (PC3), and future studies will be required to determine whether similar effects are observed in additional prostate cancer models with distinct molecular features (e.g., DU145 and androgen-responsive cell lines), thereby strengthening the generalizability of these findings. Although preliminary viability experiments in non-tumorigenic PNT2 cells suggested differential sensitivity under the tested conditions, comprehensive evaluation of tumor selectivity and pathway-specific modulation in normal prostate epithelial models will require dedicated investigation.

The chemical characterization of the *Moringa oleifera* extract was based on semi-quantitative GC–MS analysis of the detectable lipid fraction. Although stearic acid was identified as a pragmatic operational reference marker to improve batch reproducibility, further quantitative standardization and identification of additional bioactive constituents will be necessary to support translational development.

The concentrations used in this in vitro study should be regarded as proof-of-concept conditions and are not intended to reflect achievable in vivo exposure levels. Although 100 μg/mL was selected based on preserved metabolic activity and consistent pathway-associated modulation, further studies will be necessary to assess pharmacological feasibility at lower doses, in more complex biological systems, and using isolated or chemically defined fractions.

Finally, although MMP-2 and MMP-9 are widely described as relevant mediators of prostate cancer invasion, their transcriptional modulation was not prominent under our specific experimental conditions, reinforcing the concept that protease regulation in prostate cancer is highly context-dependent and influenced by cellular background and experimental settings.

5. Conclusions

This study provides evidence that exposure to a semi-characterized *Moringa oleifera* ethanolic extract is associated with multi-level biological effects in AR-negative PC3 prostate cancer cells, including modulation of the IGF-1/IGF1R signaling axis and downstream pathways. Under the applied experimental conditions, the extract reduced cell migration, promoted G0/G1 cell cycle accumulation, increased apoptotic cell death, and was associated with decreased expression of mesenchymal markers and extracellular matrix remodeling mediators.

At the molecular level, *Moringa oleifera* exposure was associated with reduced IGF1R expression and phosphorylation, attenuation of AKT and ERK signaling, modulation of integrins α2/β1, and altered transcription of ECM-related mediators, including MMP13 and cathepsin B, together with increased expression of endogenous protease inhibitors. Although the canonical gelatinases MMP-2 and MMP-9 were not prominently modulated under the present experimental conditions, these findings reinforce the concept that protease regulation in prostate cancer is highly context-dependent.

The extract was characterized through semi-quantitative GC–MS analysis of its detectable lipid fraction, and stearic acid was identified as a pragmatic operational reference marker to support batch reproducibility. The concentration selected for mechanistic investi-

gation (100 µg/mL) should be interpreted as a proof-of-concept in vitro condition rather than a direct surrogate of achievable in vivo exposure levels.

Preliminary viability experiments in non-tumorigenic prostate epithelial cells suggested differential sensitivity compared with PC3 cells; however, comprehensive evaluation of tumor selectivity, pathway-specific modulation in normal cells, and translational relevance will require dedicated investigation.

Overall, the present findings indicate that *Moringa oleifera* extract is associated with modulation of signaling pathways and cellular programs relevant to aggressive, hormone-independent prostate cancer. Further studies in additional cellular models, at lower concentrations, using purified fractions, and in in vivo systems will be necessary to clarify pharmacological feasibility and potential clinical applicability.

Supplementary Materials: The following supporting information can be downloaded at: https://www.mdpi.com/article/10.3390/sci8030055/s1, Figure S1: Cytotoxicity of *Moringa oleifera* extract on PNT2 cells. Cells were exposed to increasing concentrations of extract (50, 100, 200, 300, 1500 and 2000 µg/mL) for 24 h. Cell viabilities were measured via MTT assay. Data are presented as mean ± SD from three independent biological replicates. Statistical analysis was performed using one-way ANOVA followed by Dunnett's post hoc test, (** $p < 0.01$ vs. Ctrl); Figure S2: Light microscopy images of PC3 cells under different experimental conditions. (A) PC3 cells + 1 µM NVP-AEW541 hydrochloride; (B) PC3 cells + 1 µM NVP-AEW541 hydrochloride + 50 ng/mL IGF-I; (C) PC3 cells + 100 µg/mL *Moringa oleifera* + 50 ng/mL IGF-1; (D) PC3 cells + 100 µg/mL *Moringa oleifera* + 1 µM NVP-AEW541 hydrochloride + 50 ng/mL IGF-I. Images are representative of three independent experiments, each performed in triplicate. Original magnification: 4×; Figure S3: Flow cytometry dot plot showing cell cycle analysis based on DNA content (FL2-A) versus side scatter (SSC-H). The fluorescence intensity (FL2-A) corresponds to DNA amount, allowing discrimination of cells in different phases of the cell cycle. Side scatter (SSC-H) provides information on cell granularity and complexity. (A) PC3 cells + 1 µM NVP-AEW541 hydrochloride; (B) PC3 cells + 1 µM NVP-AEW541 hydrochloride + 50 ng/mL IGF-I; (C) PC3 cells + 100 µg/mL *Moringa oleifera* + 50 ng/mL IGF-1; (D) PC3 cells + 100 µg/mL *Moringa oleifera* + 1 µM NVP-AEW541 hydrochloride + 50 ng/mL IGF-I; Figure S4: Flow cytometry histogram showing cell cycle distribution based on DNA content (FL2-A). The peaks represent different phases of the cell cycle: Sub G1 (apoptotic cells with fragmented DNA), G0/G1 (resting or initial phase with diploid DNA content), S phase (DNA synthesis), and G2/M (cells with replicated DNA preparing for mitosis). (A) Control/Ctrl, (B) PC3 cells + 100 µg/mL *Moringa oleifera*; Figure S5: Flow cytometry dot plot showing Annexin V-FITC (FL1-H) versus Propidium Iodide (PI, FL2-H) staining of cells. The four quadrants represent different cell populations: live cells (Annexin V-/PI-), early apoptotic cells (Annexin V+/PI-), late apoptotic or necrotic cells (Annexin V+/PI+), and necrotic/dead cells (Annexin V-/PI+). (A) PC3 cells + 1 µM NVP-AEW541 hydrochloride; (B) PC3 cells + 1 µM NVP-AEW541 hydrochloride + 50 ng/mL IGF-I; (C) PC3 cells + 100 µg/mL *Moringa oleifera* + 50 ng/mL IGF-1; (D) PC3 cells + 100 µg/mL *Moringa oleifera* + 1 µM NVP-AEW541 hydrochloride + 50 ng/mL IGF-I; Table S1: Semi-quantitative GC–MS profile of *Moringa oleifera* ethanolic extract (area normalization).

Author Contributions: Conceptualization, F.M. and T.B.; methodology, F.M.; investigation, C.L., C.B., V.C., A.S., C.G., L.P. and M.C.; cell cultures and functional assays (MTT, scratch, Western blot), C.L., L.P. and M.C.; RT-PCR analysis, C.B.; flow cytometry analysis, A.S.; gas chromatography–mass spectrometry analysis and data interpretation, C.G.; software and data analysis, C.L., C.B., A.S., L.P. and M.C.; formal analysis, F.M. and T.B.; data curation, F.M.; visualization and final figures, F.M.; resources, G.L. and T.B.; writing—original draft preparation, F.M. and T.B.; writing—review and editing, F.M., G.L. and T.B.; supervision, F.M. and T.B.; project administration, F.M. and T.B.; funding acquisition, G.L. and T.B. All authors have read and agreed to the published version of the manuscript.

Funding: This research received no external funding.

Institutional Review Board Statement: Not applicable.

Informed Consent Statement: Not applicable.

Data Availability Statement: The data presented in this study are available from the authors upon reasonable request.

Conflicts of Interest: The authors declare no conflicts of interest.

References

1. Siegel, R.L.; Miller, K.D.; Jemal, A. Cancer Statistics, 2020. *CA Cancer J. Clin.* **2020**, *70*, 7–30. [CrossRef]
2. Kirby, M.; Hirst, C.; Crawford, E.D. Characterising the Castration-Resistant Prostate Cancer Population: A Systematic Review. *Int. J. Clin. Pract.* **2011**, *65*, 1180–1192. [CrossRef]
3. Kaighn, M.E.; Narayan, K.S.; Ohnuki, Y.; Lechner, J.F.; Jones, L.W. Establishment and Characterization of a Human Prostatic Carcinoma Cell Line (PC-3). *Investig. Urol.* **1979**, *17*, 16–23. [PubMed]
4. Tai, S.; Sun, Y.; Squires, J.M.; Zhang, H.; Oh, W.K.; Liang, C.Z.; Huang, J. PC3 Is a Cell Line Characteristic of Prostatic Small Cell Carcinoma. *Prostate* **2011**, *71*, 1668–1679. [CrossRef]
5. Tilley, W.D.; Wilson, C.M.; Marcelli, M.; McPhaul, M.J. Androgen Receptor Gene Expression in Human Prostate Carcinoma Cell Lines. *Cancer Res.* **1990**, *50*, 5382–5386. [PubMed]
6. Cham, J.; Venkateswaran, A.R.; Bhangoo, M. Targeting the PI3K-AKT-mTOR Pathway in Castration Resistant Prostate Cancer: A Review Article. *Clin. Genitourin. Cancer* **2021**, *19*, 563.e1–563.e7. [CrossRef]
7. Kohno, M.; Pouysségur, J. Targeting the ERK Signaling Pathway in Cancer Therapy. *Ann. Med.* **2006**, *38*, 200–211. [CrossRef] [PubMed]
8. Liu, Y.M.; Wu, A.D.; Chen, Y.; Ma, T.F.; Dong, B.Z.; She, Z.G.; Yi, M.L.; Mao, W.M. Gastrodin Inhibits Prostate Cancer Proliferation by Targeting Canonical Wnt/β-Catenin Signaling Pathway. *Med. Oncol.* **2023**, *41*, 32. [CrossRef] [PubMed]
9. Wang, C.; Chen, Q.; Xu, H. Wnt/β-Catenin Signal Transduction Pathway in Prostate Cancer and Associated Drug Resistance. *Discov. Oncol.* **2021**, *12*, 40. [CrossRef] [PubMed]
10. Clézardin, P.; Coleman, R.; Puppo, M.; Ottewell, P.; Bonnelye, E.; Paycha, F.; Confavreux, C.B.; Holen, I. Bone Metastasis: Mechanisms, Therapies, and Biomarkers. *Physiol. Rev.* **2021**, *101*, 797–855. [CrossRef]
11. Anwar, F.; Latif, S.; Ashraf, M.; Gilani, A.H. Moringa oleifera: A Food Plant with Multiple Medicinal Uses. *Phytother. Res.* **2007**, *21*, 17–25. [CrossRef]
12. Gopalakrishnan, L.; Doriya, K.; Kumar, D.S. Moringa oleifera: A Review on Nutritive Importance and Its Medicinal Application. *Food Sci. Hum. Wellness* **2016**, *5*, 49–56. [CrossRef]
13. Moura, M.C.; Napoleão, T.H.; Coriolano, M.C.; Paiva, P.M.; Figueiredo, R.C.; Coelho, L.C. Water-Soluble Moringa oleifera Lectin Interferes with Growth, Survival and Cell Permeability of Pathogenic Bacteria. *J. Appl. Microbiol.* **2015**, *119*, 666–676. [CrossRef] [PubMed]
14. Moura, M.C.; Trentin, D.S.; Napoleão, T.H.; Primon-Barros, M.; Xavier, A.S.; Carneiro, N.P.; Paiva, P.M.G.; Macedo, A.J.; Coelho, L.C.B.B. Multi-Effect of the Water-Soluble *Moringa oleifera* Lectin Against *Serratia marcescens* and *Bacillus* sp.: Antibacterial, Antibiofilm and Anti-Adhesive Properties. *J. Appl. Microbiol.* **2017**, *123*, 861–874. [CrossRef] [PubMed]
15. Mohd Sahardi, N.F.N.; Makpol, S. Suppression of Inflamm-Aging by Moringa oleifera and Zingiber officinale Roscoe in the Prevention of Degenerative Diseases: Evidence Review. *Molecules* **2023**, *28*, 5867. [CrossRef] [PubMed]
16. Al-Asmari, A.K.; Albalawi, S.M.; Athar, M.T.; Khan, A.Q.; Al-Shahrani, H.; Islam, M. Moringa oleifera as an Anti-Cancer Agent Against Breast and Colorectal Cancer Cell Lines. *PLoS ONE* **2015**, *10*, e0135814. [CrossRef]
17. Antonini, E.; Iori, R.; Ninfali, P.; Scarpa, E.S. Combination of Moringin and Avenanthramide 2f Inhibits Hep3B Cancer Cells via Apoptosis. *Nutr. Cancer* **2018**, *70*, 1159–1165. [CrossRef]
18. Pareek, A.; Pant, M.; Gupta, M.M.; Kashania, P.; Ratan, Y.; Jain, V.; Pareek, A.; Chuturgoon, A.A. Moringa oleifera: An Updated Comprehensive Review. *Int. J. Mol. Sci.* **2023**, *24*, 2098. [CrossRef]
19. Shahbaz, M.; Naeem, H.; Batool, M.; Imran, M.; Hussain, M.; Mujtaba, A.; Alsagaby, S.A.; Al Abdulmonem, W.; El-Ghorab, A.H.; Ghoneim, M.M.; et al. Antioxidant, Anticancer, and Anti-Inflammatory Potential of Moringa Seed and Oil. *Food Sci. Nutr.* **2024**, *12*, 6157–6173. [CrossRef]
20. Abd Karim, N.A.; Adam, A.H.B.; Jaafaru, M.S.; Rukayadi, Y.; Abdull Razis, A.F. Apoptotic Potential of GMG-ITC from Moringa oleifera Seeds on PC-3 Cells. *Molecules* **2023**, *28*, 3214. [CrossRef]
21. Jung, I.L. Soluble Extract from Moringa oleifera Leaves with New Anticancer Activity. *PLoS ONE* **2014**, *9*, e000000. [CrossRef]
22. Khan, F.; Pandey, P.; Ahmad, V.; Upadhyay, T.K. Moringa Methanolic Extract Induces Apoptosis and G0/G1 Arrest in PC3. *J. Food Biochem.* **2020**, *44*, e13338. [CrossRef]
23. Xie, J.; Luo, F.-X.; Shi, C.-Y.; Jiang, W.-W.; Qian, Y.-Y.; Yang, M.-R.; Song, S.; Dai, T.-Y.; Peng, L.; Gao, X.-Y.; et al. Moringa oleifera Alkaloids Inhibit PC3 Growth and Migration via Wnt/β-Catenin/COX-2. *Front. Pharmacol.* **2020**, *11*, 523962, Erratum in *Front Pharmacol.* **2021**, *12*, 760933. https://doi.org/10.3389/fphar.2021.760933. [CrossRef]
24. Adzavon, Y.M.; Culig, Z.; Sun, Z. Interactions Between Androgen and IGF1 Axes in Prostate Tumorigenesis. *Nat. Rev. Urol.* **2025**, *22*, 268–275. [CrossRef]

25. Song, W.H.; Kim, J.-E.; Rajbongshi, L.; Lee, S.-R.; Kim, Y.; Hwang, S.Y.; Oh, S.-O.; Kim, B.S.; Lee, D.; Yoon, S. Polydopamine-Coated Surfaces Promote Adhesion, Migration, Proliferation, Chemoresistance, Stemness, and Epithelial–Mesenchymal Transition of Human Prostate Cancer Cell Lines In Vitro via Integrin α2β1–FAK–JNK Signaling. *Int. J. Mol. Sci.* **2026**, *27*, 655. [CrossRef]
26. Medina-González, A.; Eiró-Díaz, N.; Fernández-Gómez, J.M.; Ovidio-González, L.; Jalón-Monzón, A.; Casas-Nebra, J.; Escaf-Barmadah, S. Comparative analysis of the expression of metalloproteases (MMP-2, MMP-9, MMP-11 and MMP-13) and the tissue inhibitor of metalloprotease 3 (TIMP-3) between previous negative biopsies and radical prostatectomies. *Actas Urol. Esp. (Engl. Ed.)* **2020**, *44*, 78–85. [CrossRef]
27. Kalantari, E.; Abolhasani, M.; Roudi, R.; Farajollahi, M.M.; Farhad, S.; Madjd, Z.; Askarian-Amiri, S.; Mohsenzadegan, M. Co-expression of TLR-9 and MMP-13 is associated with the degree of tumour differentiation in prostate cancer. *Int. J. Exp. Pathol.* **2019**, *100*, 123–132. [CrossRef]
28. Reel, B.; Korkmaz, C.G.; Arun, M.Z.; Yildirim, G.; Ogut, D.; Kaymak, A.; Micili, S.C.; Ergur, B.U. The Regulation of Matrix Metalloproteinase Expression and the Role of Discoidin Domain Receptor 1/2 Signalling in Zoledronate-treated PC3 Cells. *J. Cancer* **2015**, *6*, 1020–1029. [CrossRef] [PubMed]
29. Liu, G.; Zhu, M.; Zhang, M.; Pan, F. Emerging Role of IGF-1 in Prostate Cancer: A Biomarker and Target. *Cancers* **2023**, *15*, 1287. [CrossRef] [PubMed]
30. Vongsak, B.; Sithisarn, P.; Mangmool, S.; Thongpraditchote, S.; Wongkrajang, Y.; Gritsanapan, W. Maximizing Total Phenolics, Total Flavonoids Contents and Antioxidant Activity of Moringa oleifera Leaf Extract by the Appropriate Extraction Method. *Ind. Crops Prod.* **2013**, *44*, 566–571. [CrossRef]
31. Fregonese, M.; Albino, A.; Covino, C.; Gili, A.; Bacci, M.; Nicoletti, A.; Gambelunghe, C. Drug Checking as Strategy for Harm Reduction in Recreational Contests: Evaluation of Two Different Drug Analysis Methodologies. *Front Psychiatry* **2021**, *12*, 596895. [CrossRef] [PubMed]
32. Vang Mouritzen, M.; Jenssen, H. Optimized Scratch Assay for In Vitro Testing of Cell Migration with an Automated Optical Camera. *J. Vis. Exp.* **2018**, *138*, 57691. [CrossRef]
33. Mancuso, F.; Arato, I.; Bellucci, C.; Lilli, C.; Eugeni, E.; Aglietti, M.C.; Stabile, A.M.; Pistilli, A.; Brancorsini, S.; Gaggia, F.; et al. Zinc restores functionality in porcine prepubertal Sertoli cells exposed to subtoxic cadmium concentration via regulating the Nrf2 signaling pathway. *Front. Endocrinol.* **2023**, *14*, 962519. [CrossRef]
34. Baroni, T.; Lilli, C.; Bellucci, C.; Luca, G.; Mancuso, F.; Fallarino, F.; Falabella, G.; Arato, I.; Calvitti, M.; Marinucci, L.; et al. In vitro cadmium effects on ECM gene expression in human bronchial epithelial cells. *Cytokine* **2015**, *72*, 9–16. [CrossRef] [PubMed]
35. Cannarella, R.; Mancuso, F.; Condorelli, R.A.; Arato, I.; Mongioì, L.M.; Giacone, F.; Lilli, C.; Bellucci, C.; La Vignera, S.; Calafiore, R.; et al. Effects of GH and IGF1 on Basal and FSH-Modulated Porcine Sertoli Cells In-Vitro. *J. Clin. Med.* **2019**, *8*, 811. [CrossRef] [PubMed]
36. Arato, I.; Giovagnoli, S.; Roscini, L.; Calvitti, M.; Bellucci, C.; Lilli, C.; Eugeni, E.; Brancorsini, S.; Cardinali, G.; Luca, G.; et al. Exploring Sertoli Cells' Innate Bulwark Role Against Infections: In Vitro Performances on *Candida tropicalis* Biofilms. *Cells* **2025**, *14*, 495. [CrossRef]
37. Lappano, R.; Sebastiani, A.; Cirillo, F.; Rigiracciolo, D.C.; Galli, G.R.; Curcio, R.; Malaguarnera, R.; Belfiore, A.; Cappello, A.R.; Maggiolini, M. The Lauric Acid-Activated Signaling Prompts Apoptosis in Cancer Cells. *Cell Death Discov.* **2017**, *3*, 17063. [CrossRef]
38. Dailey, O.D., Jr.; Wang, X.; Chen, F.; Huang, G. Anticancer Activity of Oleic-Acid Derivatives. *Anticancer Res.* **2011**, *31*, 3165–3169. [PubMed]
39. Niu, L.; Li, W.; Chen, X.; Su, X.; Dong, J.; Liao, Q.; Zhou, X.; Shi, S.; Sun, R. 1-Monopalmitin Promotes Apoptosis Through PI3K/Akt. *Environ. Toxicol.* **2023**, *38*, 2621–2631. [CrossRef]
40. Guo, W.; Giancotti, F.G. Integrin Signalling During Tumour Progression. *Nat. Rev. Mol. Cell Biol.* **2004**, *5*, 816–826. [CrossRef]
41. Gurel, B.; Iwata, T.; Koh, C.M.; Jenkins, R.B.; Lan, F.; van Dang, C.; Hicks, J.L.; Morgan, J.; Cornish, T.C.; Sutcliffe, S.; et al. Nuclear MYC Protein Overexpression is an early alteration in human Prostate Carcinogenesis. *Mod. Pathol.* **2008**, *21*, 1156–1167. [CrossRef]
42. Khan, M.Z.; Zugaza, J.L.; Torres Aleman, I. The Signaling Landscape of IGF-1. *J. Biol. Chem.* **2025**, *301*, 108047. [CrossRef] [PubMed]
43. Ma, Q.L.; Yang, T.L.; Yin, J.Y.; Peng, Z.Y.; Yu, M.; Liu, Z.Q.; Chen, F.P. Role of IGF-1 in Cell Cycle Progression. *Biochem. Biophys. Res. Commun.* **2009**, *389*, 150–155. [CrossRef]
44. Wang, Z. Cell Cycle Progression and Synchronization: An Overview. In *Methods in Molecular Biology*; Humana: New York, NY, USA, 2022. [CrossRef]
45. Zumsteg, A.; Caviezel, C.; Pisarsky, L.; Strittmatter, K.; García-Echeverría, C.; Hofmann, F.; Christofori, G. Repression of Malignant Tumor Progression upon Pharmacologic IGF1R Blockade in a Mouse Model of Insulinoma. *Mol. Cancer Res.* **2012**, *10*, 800–809. [CrossRef]
46. Elmore, S. Apoptosis: A Review of Programmed Cell Death. *Toxicol. Pathol.* **2007**, *35*, 495–516. [CrossRef]
47. Martinucci, B.; Cucielo, M.S.; Minatel, B.C.; Cury, S.S.; Caxali, G.H.; Aal, M.C.E.; Felisbino, S.L.; Pinhal, D.; Carvalho, R.F.; Delella, F.K. Fibronectin Modulates the Expression of miRNAs in Prostate Cancer Cell Lines. *Front. Vet. Sci.* **2022**, *9*, 879997. [CrossRef]
48. Satelli, A.; Li, S. Vimentin in cancer and its potential as a molecular target for cancer therapy. *Cell. Mol. Life Sci.* **2011**, *68*, 3033–3046. [CrossRef]
49. Cao, Z.Q.; Wang, Z.; Leng, P. Aberrant N-cadherin expression in cancer. *Biomed Pharmacother.* **2019**, *118*, 109320. [CrossRef] [PubMed]

50. Mansor, R.; Holly, J.; Barker, R.; Biernacka, K.; Zielinska, H.; Koupparis, A.; Rowe, E.; Oxley, J.; Sewell, A.; Martin, R.M.; et al. IGF-1 and Hyperglycaemia-induced FOXA1 and IGFBP-2 affect epithelial to mesenchymal transition in Prostate epithelial Cells. *Oncotarget* **2020**, *11*, 2543–2559. [CrossRef]
51. Osanai, M.; Murata, M.; Nishikiori, N.; Chiba, H.; Kojima, T.; Sawada, N. Epigenetic Silencing of Occludin Promotes Tumorigenic and Metastatic Properties. *Cancer Res.* **2006**, *66*, 9125–9133. [CrossRef] [PubMed]
52. Yang, C.; Liu, Y.; Hu, Y.; Fang, L.; Huang, Z.; Cui, H.; Xie, J.; Hong, Y.; Chen, W.; Xiao, N.; et al. Myc Inhibition Tips the immune balance to Promote Antitumor Immunity. *Cell Mol. Immunol.* **2022**, *19*, 1030–1041. [CrossRef] [PubMed]
53. Mijanović, O.; Branković, A.; Panin, A.N.; Savchuk, S.; Timashev, P.; Ulasov, I.; Lesniak, M. Cathepsin B: A Sellsword of Cancer Progression. *Cancer Lett.* **2019**, *449*, 207–214. [CrossRef] [PubMed]
54. Li, S.; Pritchard, D.M.; Yu, L.-G. MMP-13 in Cancer Progression. *Cancers* **2022**, *14*, 3263. [CrossRef]
55. Rivenbark, A.G.; Coleman, W.B. Epigenetic regulation of cystatins in cancer. *Front. Biosci. (Landmark Ed.)* **2009**, *14*, 453–462. [CrossRef]
56. Gardner, T.A.; Lee, S.J.; Lee, S.D.; Li, X.; Shirakawa, T.; Kwon, D.D.; Park, R.Y.; Ahn, K.Y.; Jung, C. Differential Expression of Osteocalcin During Metastatic Progression. *Oncol. Rep.* **2009**, *21*, 903–908. [CrossRef] [PubMed]
57. Rodríguez-Berriguete, G.; Fraile, B.; Martínez-Onsurbe, P.; Olmedilla, G.; Paniagua, R.; Royuela, M. MAP Kinases and Prostate Cancer. *J. Signal Transduct.* **2012**, *2012*, 169170. [CrossRef] [PubMed] [PubMed Central]
58. Shorning, B.Y.; Dass, M.S.; Smalley, M.J.; Pearson, H.B. The PI3K-AKT-mTOR Pathway and Prostate Cancer: At the Crossroads of AR, MAPK, and WNT Signaling. *Int. J. Mol. Sci.* **2020**, *21*, 4507. [CrossRef]
59. Glaviano, A.; Foo, A.S.C.; Lam, H.Y.; Yap, K.C.H.; Jacot, W.; Jones, R.H.; Eng, H.; Nair, M.G.; Makvandi, P.; Geoerger, B.; et al. PI3K/AKT/mTOR Signaling Transduction Pathway and Targeted Therapies in Cancer. *Mol. Cancer* **2023**, *22*, 138. [CrossRef]
60. Ayala, G.; Thompson, T.; Yang, G.; Frolov, A.; Li, R.; Scardino, P.; Ohori, M.; Wheeler, T.; Harper, W. High Levels of Phosphorylated Form of Akt-1 in Prostate Cancer and Non-Neoplastic Prostate Tissues Are Strong Predictors of Biochemical Recurrence. *Clin. Cancer Res.* **2004**, *10*, 6572–6578. [CrossRef]

Disclaimer/Publisher's Note: The statements, opinions and data contained in all publications are solely those of the individual author(s) and contributor(s) and not of MDPI and/or the editor(s). MDPI and/or the editor(s) disclaim responsibility for any injury to people or property resulting from any ideas, methods, instructions or products referred to in the content.